



2319 seen by Planck

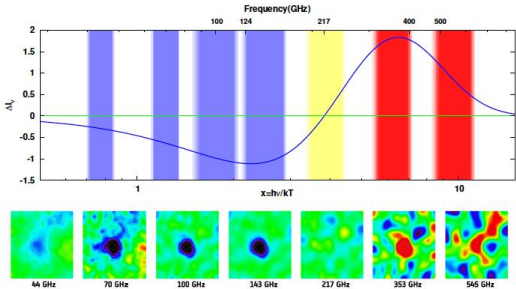
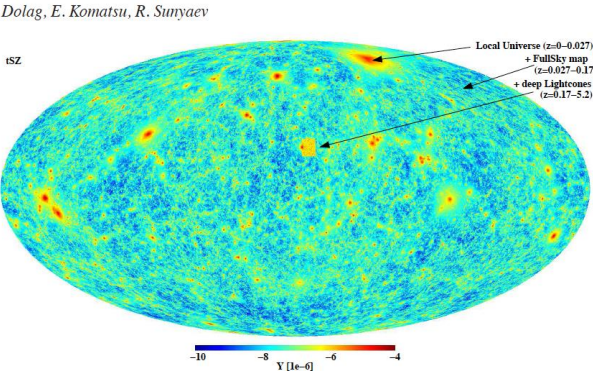


Image credit: ESA / HFI & LFI Consortia



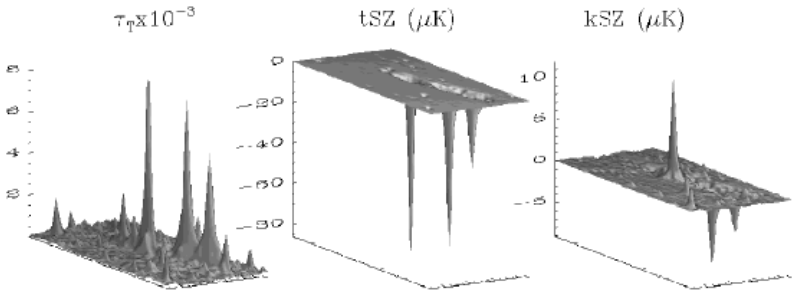
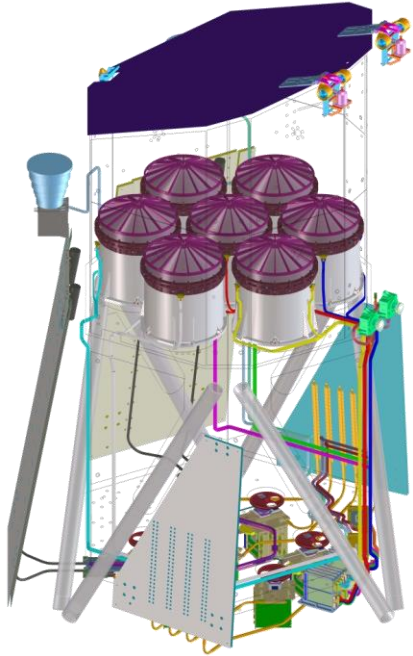
Towards a next probe
for CMB observations

CERN, Geneva

May 17, 2016

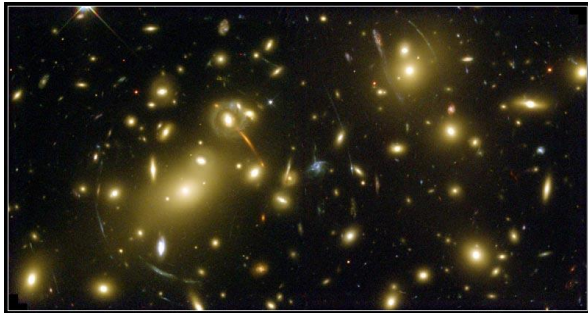
Galaxy clusters + synergy with eRosita

eRosita



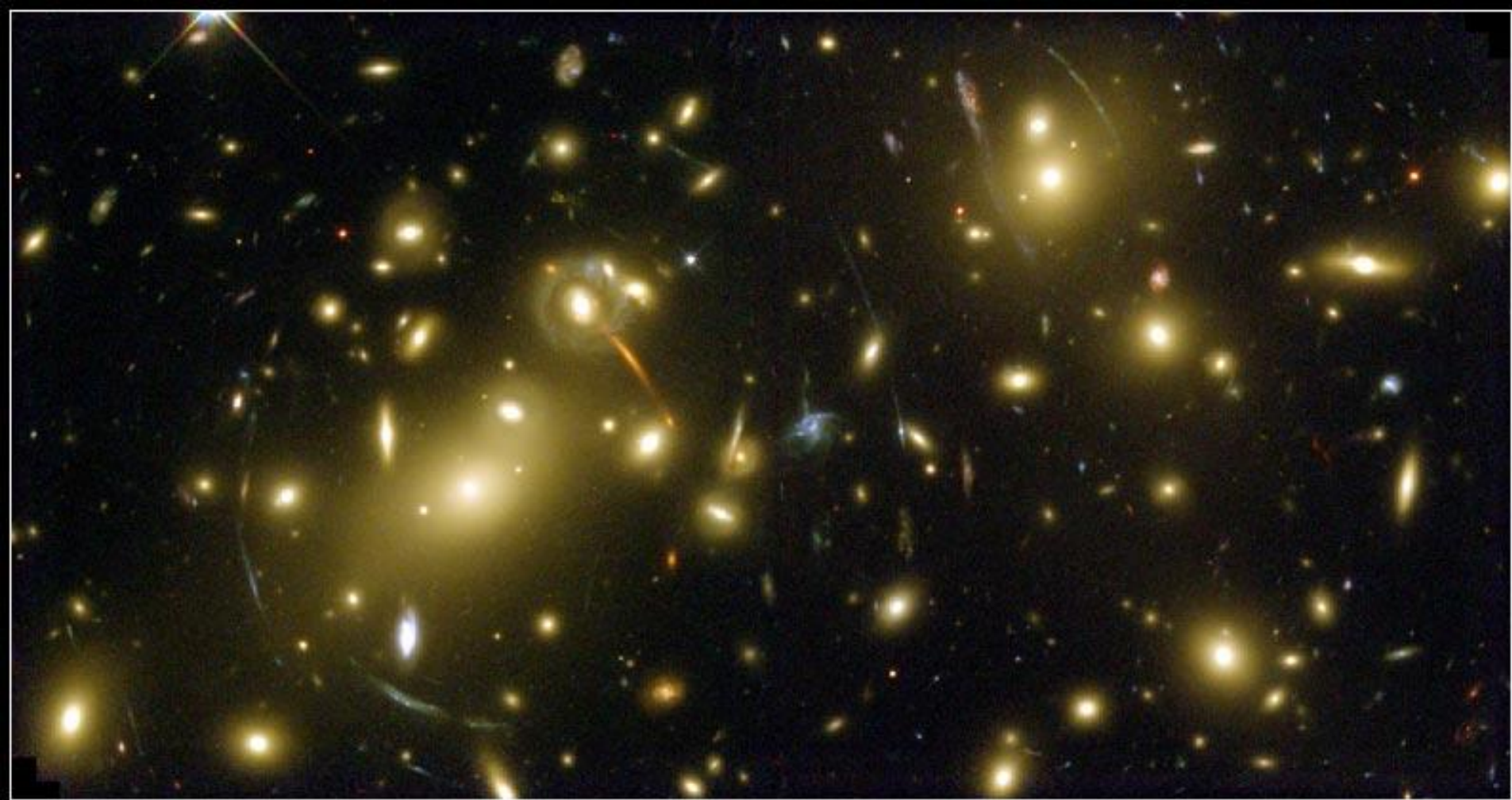
Rashid Sunyaev

Max-Planck Institut fuer Astrophysik
Space Research Institute, Moscow



Galaxy Cluster Abell 2218
NASA, A. Fruchter and the ERO Team (STScI) • STScI-PRC00-08

HST • WFPC2



Galaxy Cluster Abell 2218

HST • WFPC2

NASA, A. Fruchter and the ERO Team (STScI) • STScI-PRC00-08

Thousands of galaxies with $v \sim 1000$ km/s

Hot intergalactic gas with $T_e \sim 3 - 10$ KeV

Gravitational potential defined by
invisible *dark matter*

Distant galaxies are gravitationally *lensed* by A 2218

Major components of a galaxy cluster

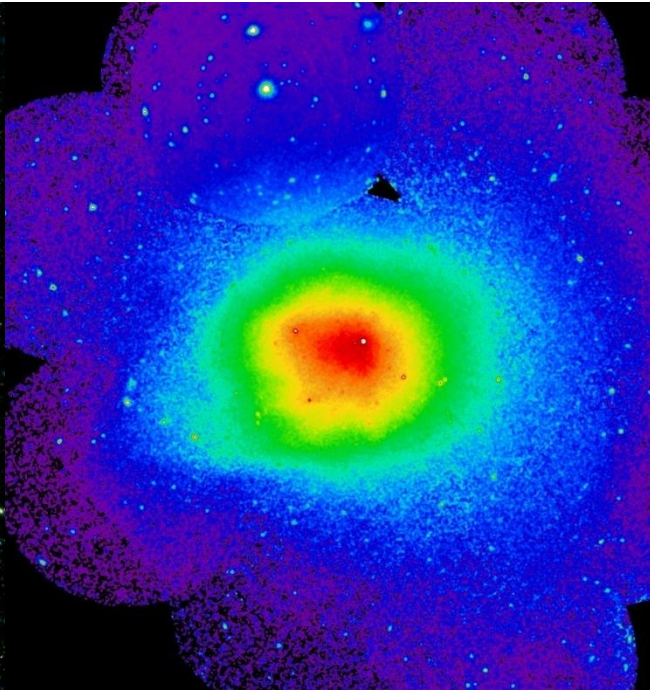
Stars



few % of total mass

Optical

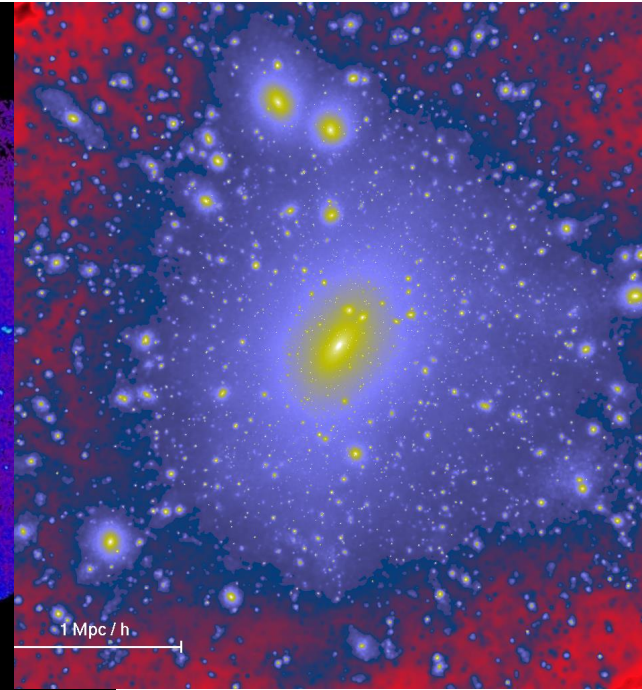
Hot gas



15 %

X-rays, CMB

Dark matter

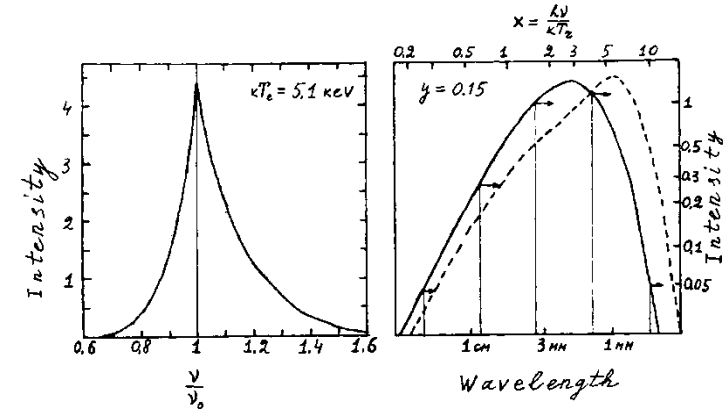


80 %

Indirect

There are three effects which make cloud visible:

1. Thermal effect (change of the CMB spectrum in the direction to the cloud with hot gas)



2. Kinetic effect (moving cloud changes the spectrum of scattered CMB photons due to Doppler effect)

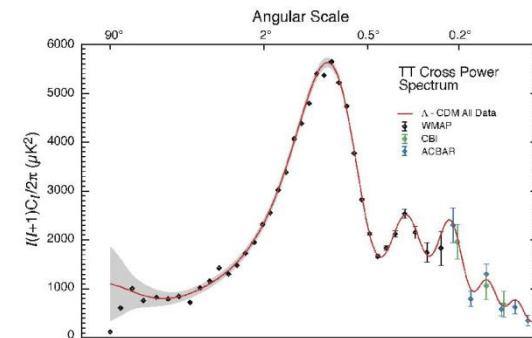
$$\frac{\Delta T}{T_r} = -\frac{v_r}{c} \tau_T$$

Full analogy with the origin of the Dipole Component in the CMB angular distribution arising due to our motion relative to the reference frame where CMB is isotropic.

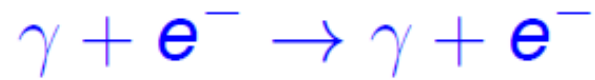
3. Blurring effect (CMB in reality is not isotropic. There are angular fluctuations. Scattering in the cloud removes all anisotropies in the direction to the cloud except 10% of quadrupole at the position of a cloud)

$$\frac{\Delta I}{I_0} = \frac{I_1(\mu) - I(\mu)}{I_0} = -\tau_T \times \left[a\mu + 0.9b(\mu^2 - \frac{1}{3}) + \sum_{n=3}^{\infty} C_n P_n(\mu) \right]$$

(see Sunyaev, Zeldovich, 1981)



Comptonization



$$\text{Doppler} : \frac{\delta\nu}{\nu} \sim \frac{v_e}{c} \sim \left(\frac{kT_e}{m_e c^2} \right)$$

$$\text{2nd order Doppler} : \left(\frac{\delta\nu}{\nu} \right)_{\text{rms}} \sim 4 \left(\frac{kT_e}{m_e c^2} \right)$$

$$\text{Recoil} : \frac{\delta\nu}{\nu} = -\frac{h\nu}{m_e c^2} (1 - \cos \theta)$$

=====

y: Amplitude of distortion

$$y = \int dt c \sigma_T n_e \frac{k_B (T_e - T_\gamma)}{m_e c^2}$$

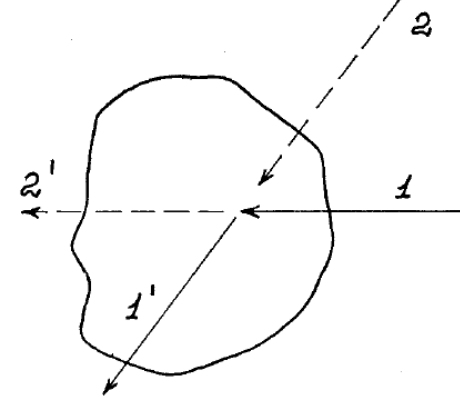
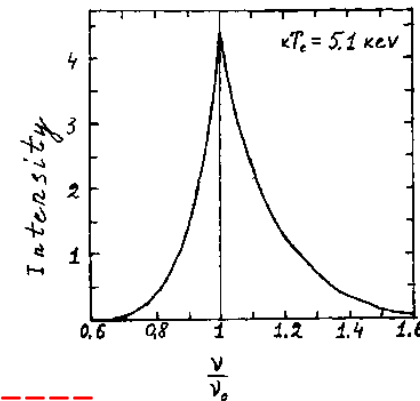
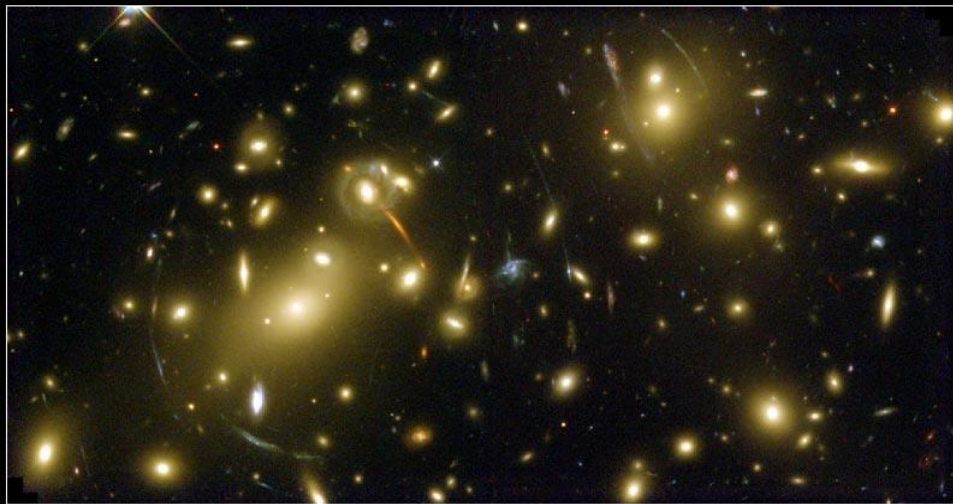


FIG. 2. The scattering of isotropic radiation field by the cloud.

Cloud is invisible





Galaxy Cluster Abell 2218
HST • WFPC2
NASA, A. Fruchter and the ERO Team (STScI) • STScI-PRC00-08

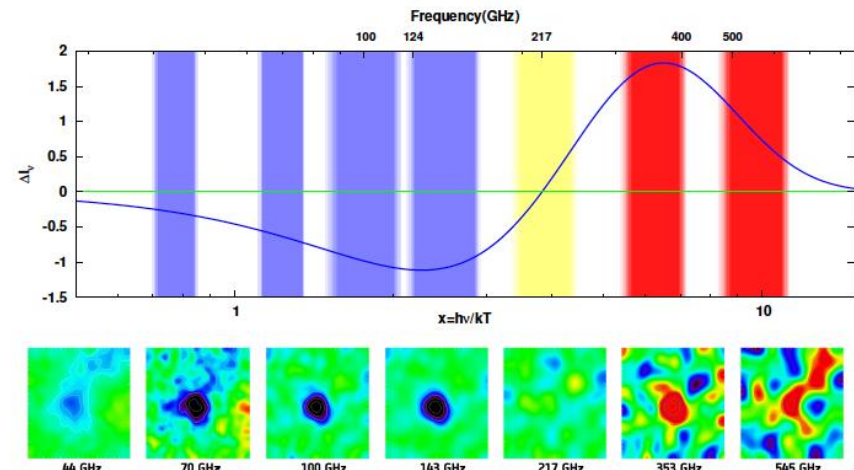


Image credit: ESA / HFI & LFI Consortia

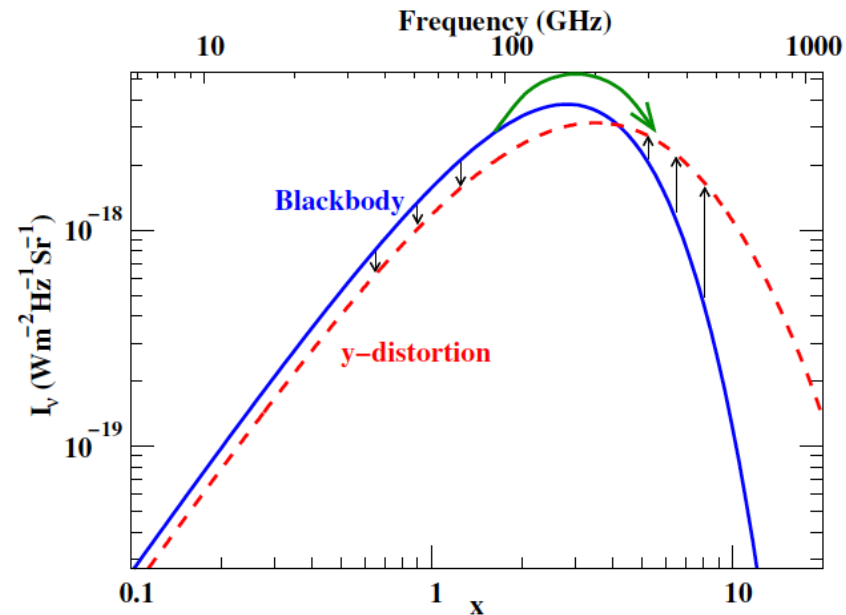
$$n_{SZ} = y T^4 \frac{\partial}{\partial T} \frac{1}{T^2} \frac{\partial n_{Pl}}{\partial T}$$

$$= y \frac{x e^x}{(e^x - 1)^2} \left(x \frac{e^x + 1}{e^x - 1} - 4 \right)$$

$$\Delta I_{sz} = I_{sz} - I_{planck} = \frac{2h\nu^3}{c^2} n_{sz}$$

(Zeldovich and Sunyaev 1969)

COBE-FIRAS limit (95%): $y \lesssim 1.5 \times 10^{-5}$ (Fixsen et al. 1996)



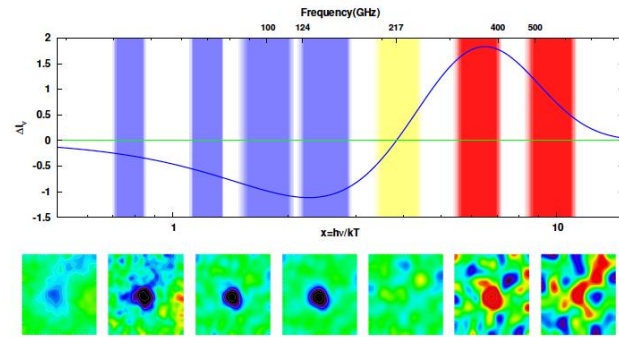
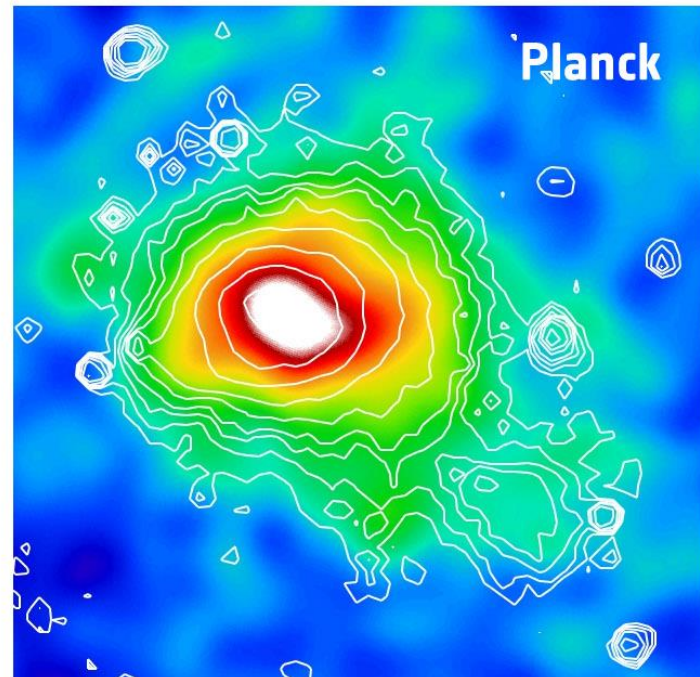
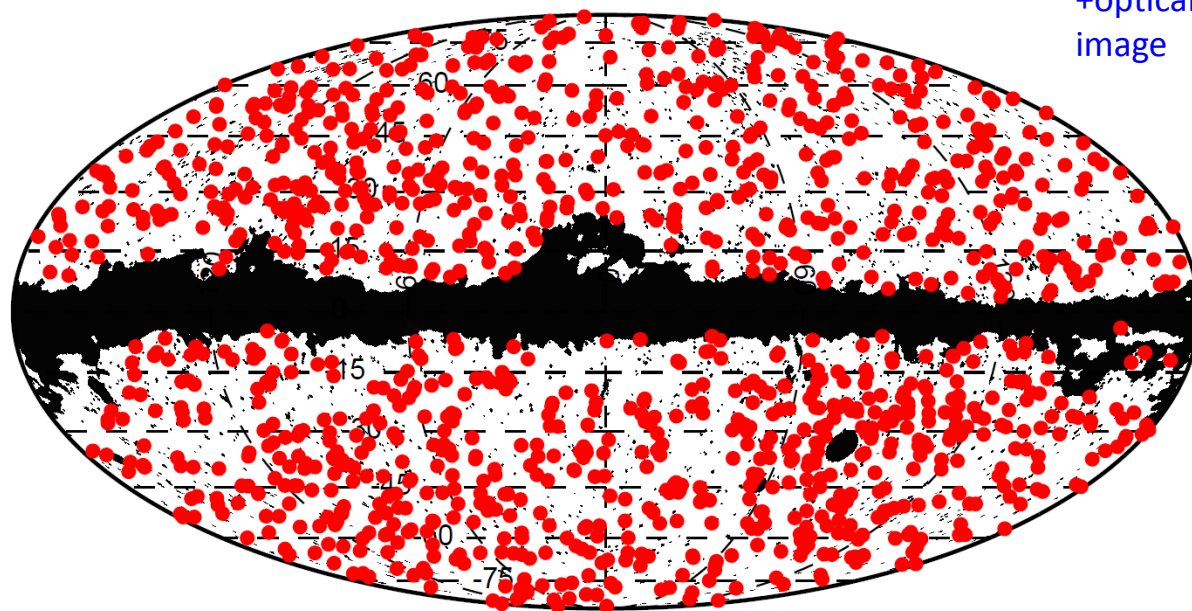


Image credit: ESA / HFI & LFI Consortia

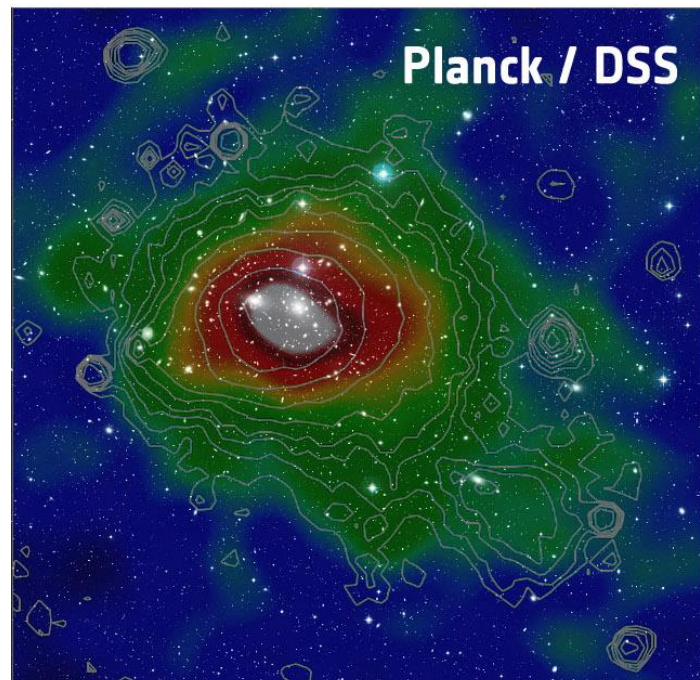
*SZ shadow,
Coma cluster
of galaxies
y-parameter map,
based on
100-857 GHz data*



*~ 900 clusters confirmed by X-Ray
or optical observations*



Planck
+optical
image



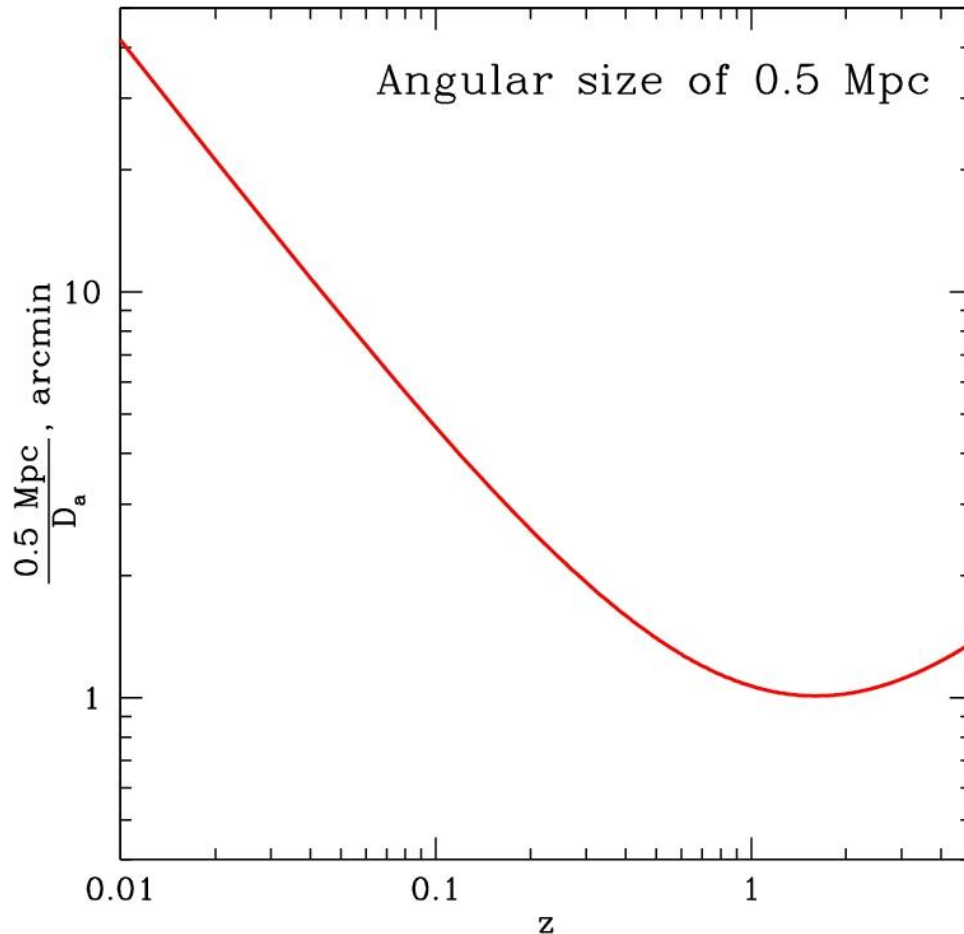
ACT and SPT

Dedicated Telescopes for measurement of
CMB polarization and fine angular scale temperature anisotropy



- Exceptional high and dry sites for dedicated CMB observations.
- Exploiting ongoing revolution in low-noise bolometer cameras

Angular size as a function of z



For distant clusters
their angular size
does not depend
on redshift!

It is close to 1 arcmin

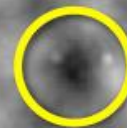
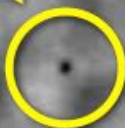
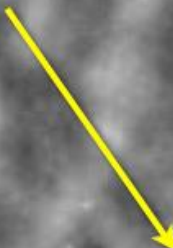
This means, that their total flux also does not depend on redshift for $0.5 < z < 2$
(for similar clusters at different redshifts)

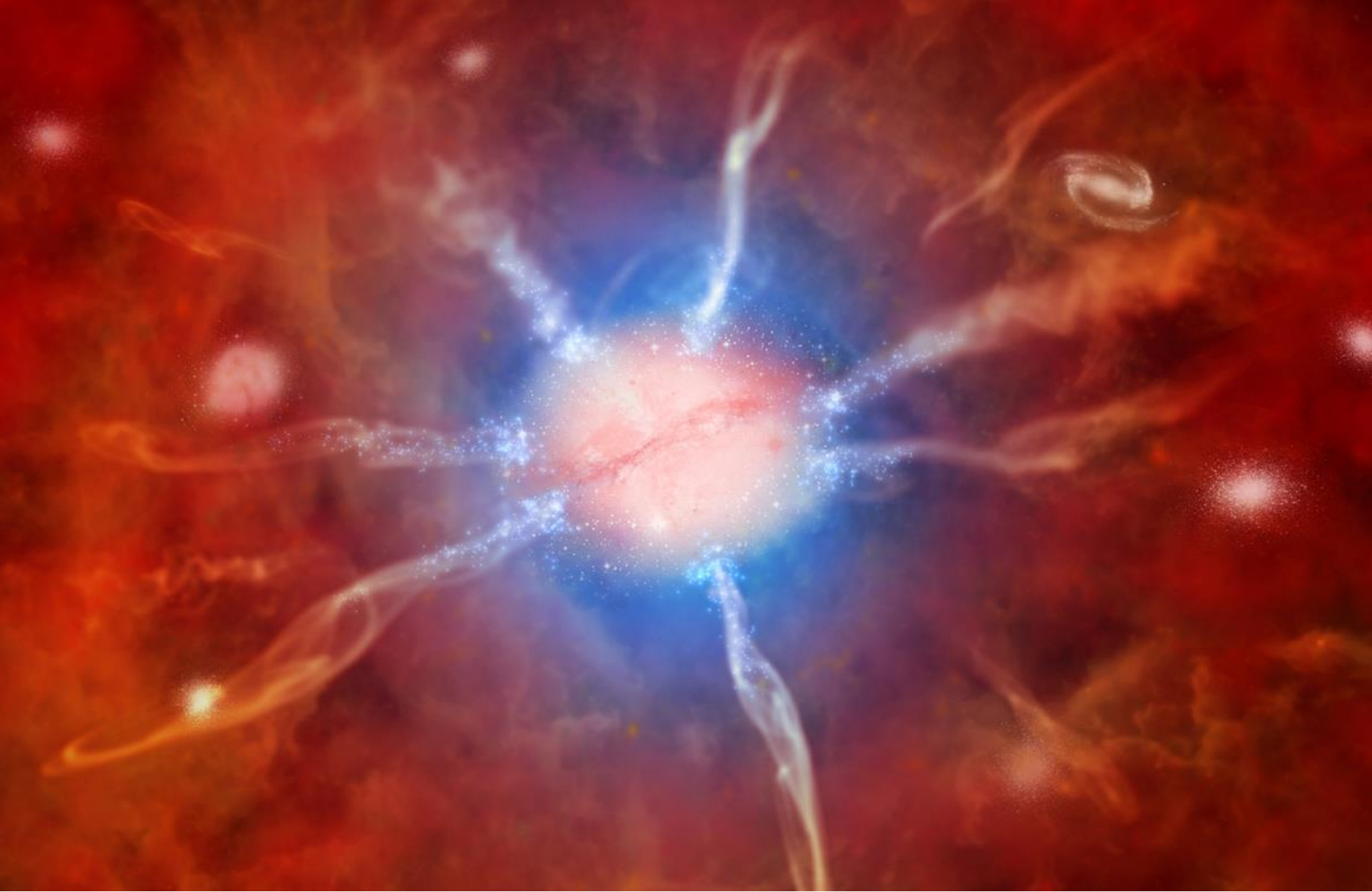
because observed surface brightness also does not depend on the redshift

SPT
150 GHz.
50 deg²

Clusters of Galaxies

"Shadows" in the microwave
background from clusters of galaxies





Fenix cluster of galaxies discovered by SPT at $z=0.596$ and observed by CHANDRA, GALEX and Magellan: star burst – 800 solar masses a year, luminosity 8×10^{45} erg/s, cooling flow ~ 3000 Solar masses a year. Black hole in the center accretes 60 solar masses a year.

Lower limit on $\langle y \rangle$ from Planck and SPT detected clusters

Sum the $\langle y \rangle$ from Planck clusters at $z < 0.3$ and SPT clusters at $z > 0.3$

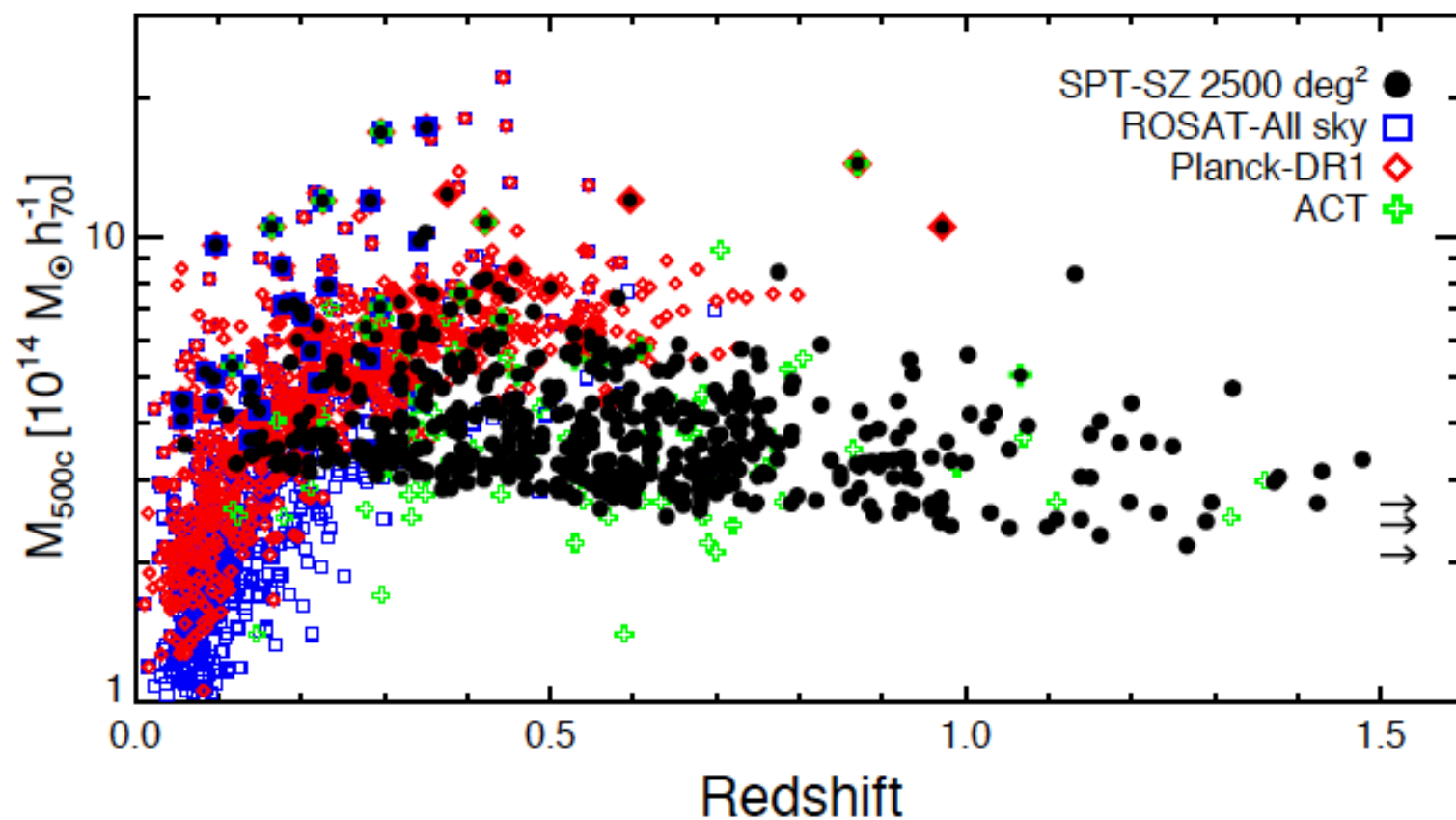


Fig. from Bleem et al. 2015 (SPT) arXiv:1409.0850

Lower limit on $\langle y \rangle$ from Planck and SPT detected clusters

Observed clusters \Rightarrow Minimum average y -distortion in the CMB

$$\langle y \rangle > 5.4 \times 10^{-8} \text{ (Khatri \& Sunyaev 2015)}$$

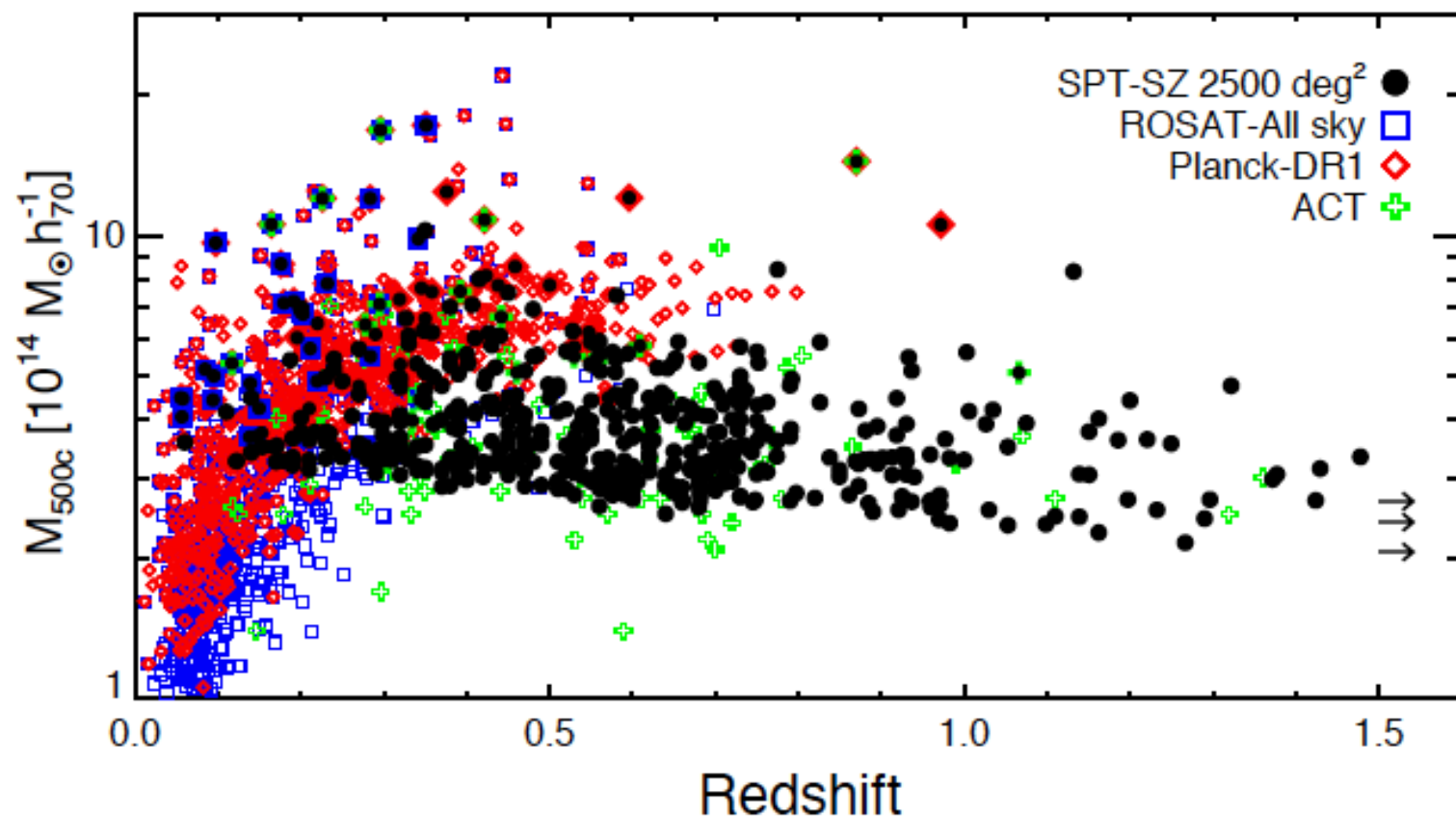


Fig. from Bleem et al. 2015 (SPT) arXiv:1409.0850

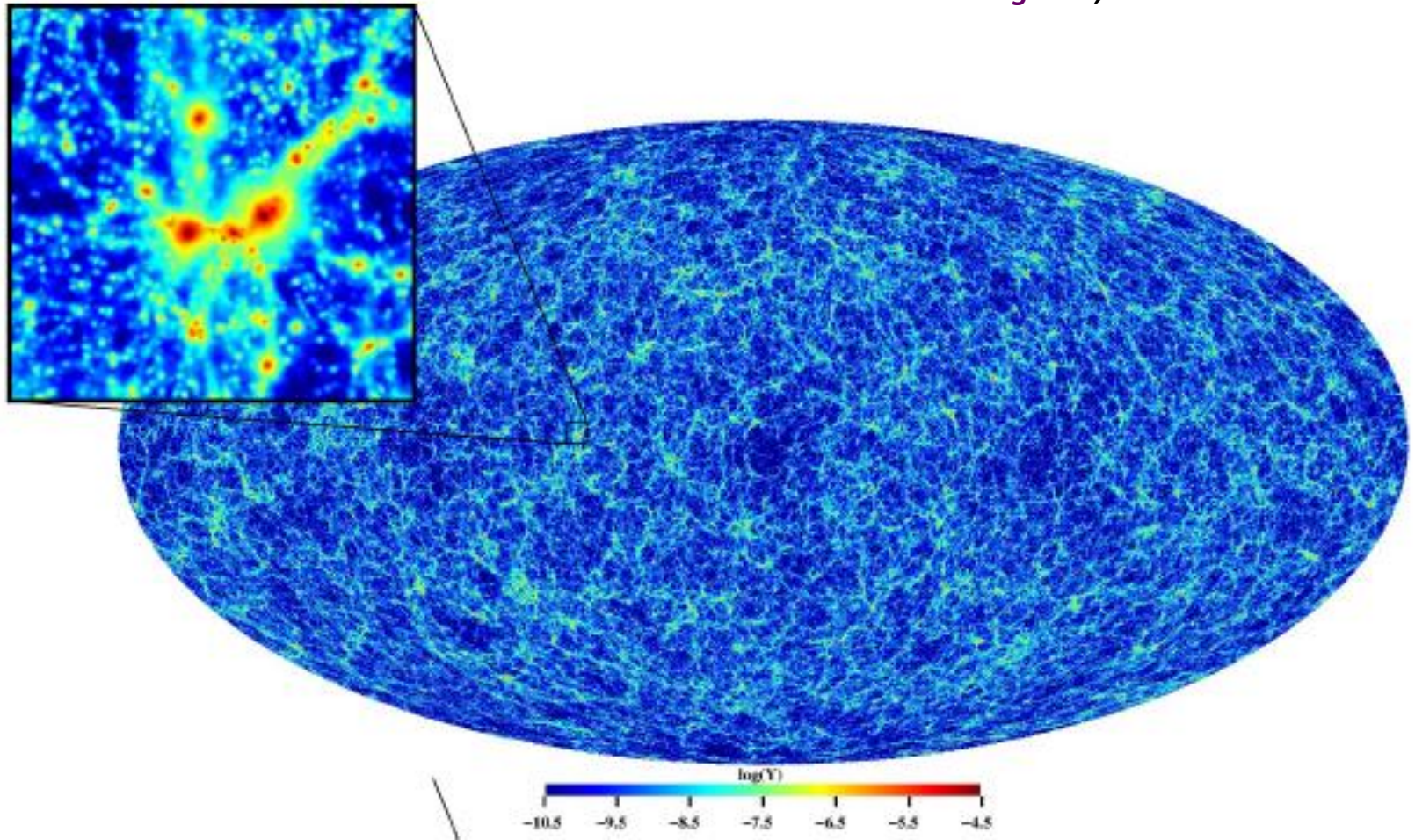


Figure 34. Map of simulated y-distortion taken from [207]. The y-type signal from the post-reionization epoch is dominated by the collapsed objects and filaments in the large scale structure.

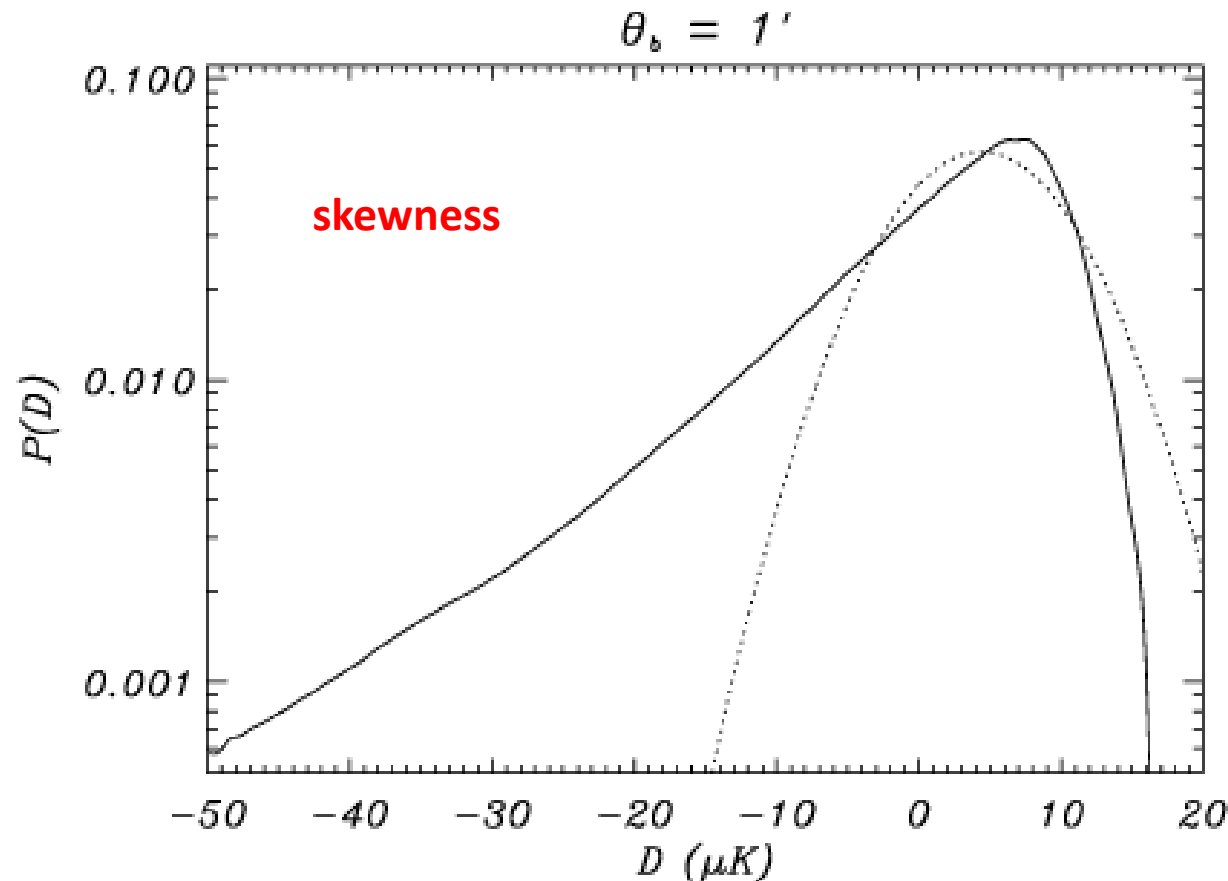
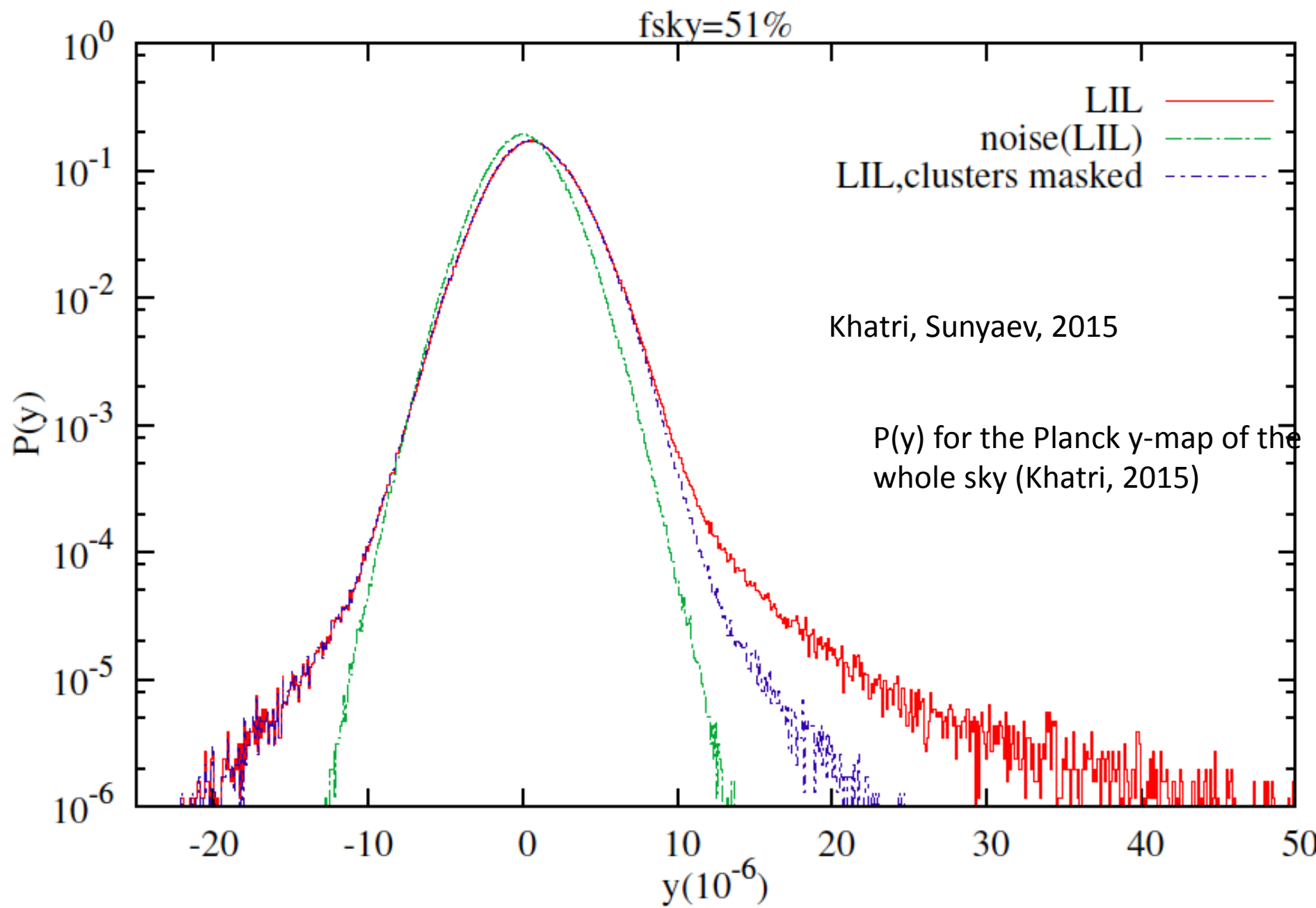


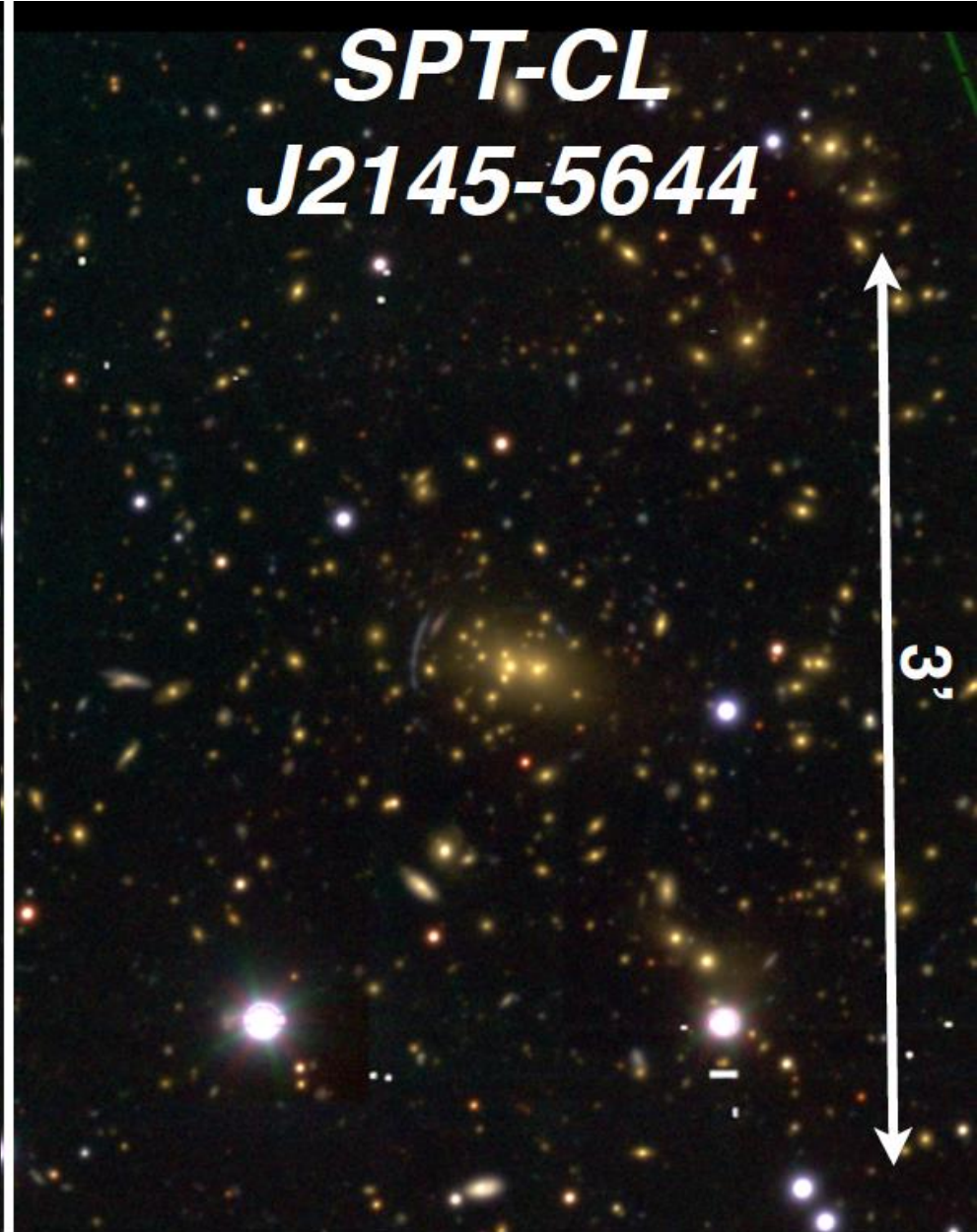
Figure 2. Example of the strong non-Gaussianity of the $P(D)$ function for SZ clusters. We present the $P(D)$ function for a SZ map in the Rayleigh–Jeans region of the spectrum, where clusters are ‘negative’ sources. For comparison, we also show the best Gaussian fit to this $P(D)$ curve ($\sigma = 6.1 \mu K$). This curve will be explained in detail in Section 7.



***SPT-CL
J2138-6008***

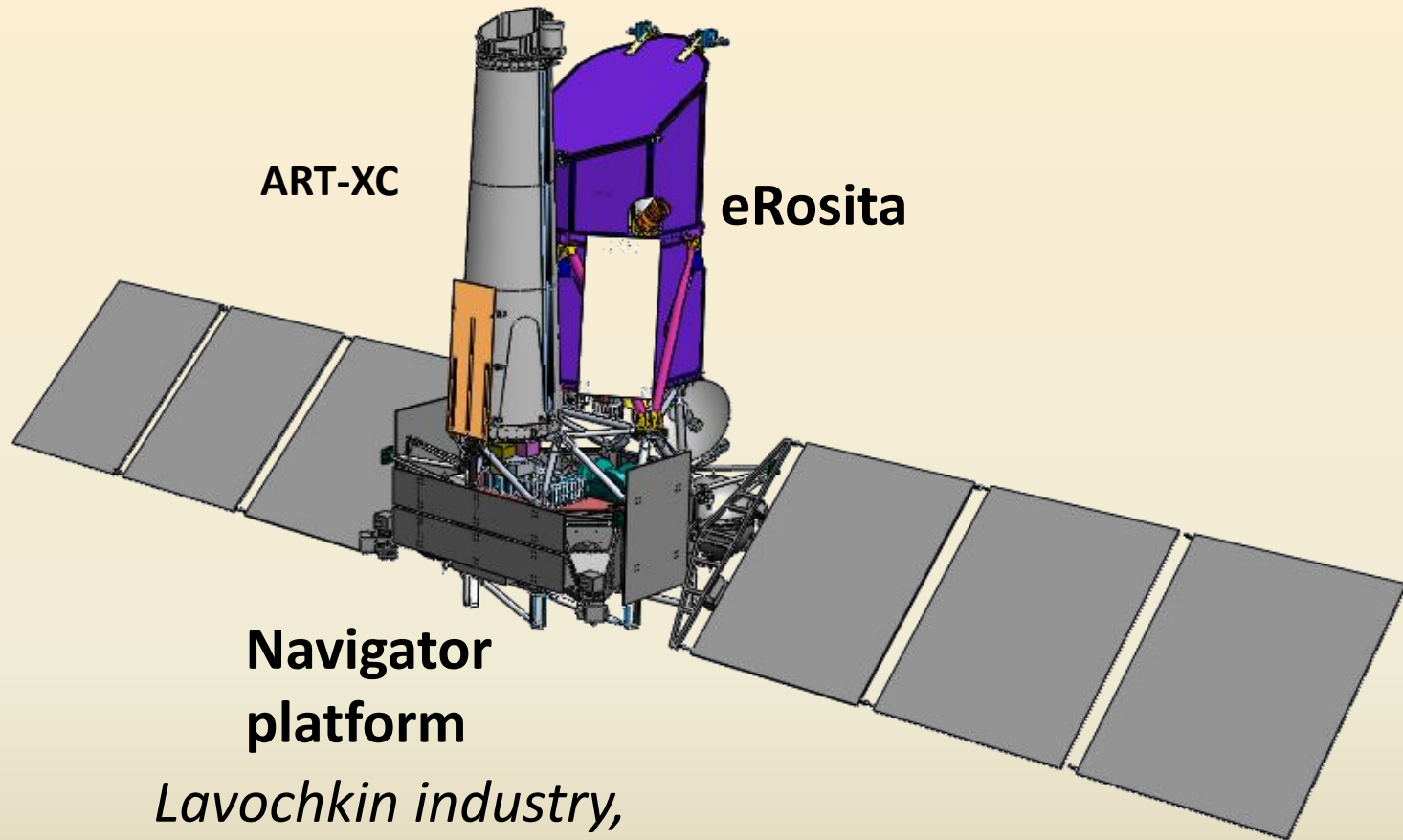


***SPT-CL
J2145-5644***



Optical follow-up; redshifts, lensing, dynamical masses

Spectrum-Roentgen-Gamma (SRG)



**Navigator
platform**

*Lavochkin industry,
Khimki near Moscow*

*Launch from Baikonur with Zenit-Fregat,
September 2017*

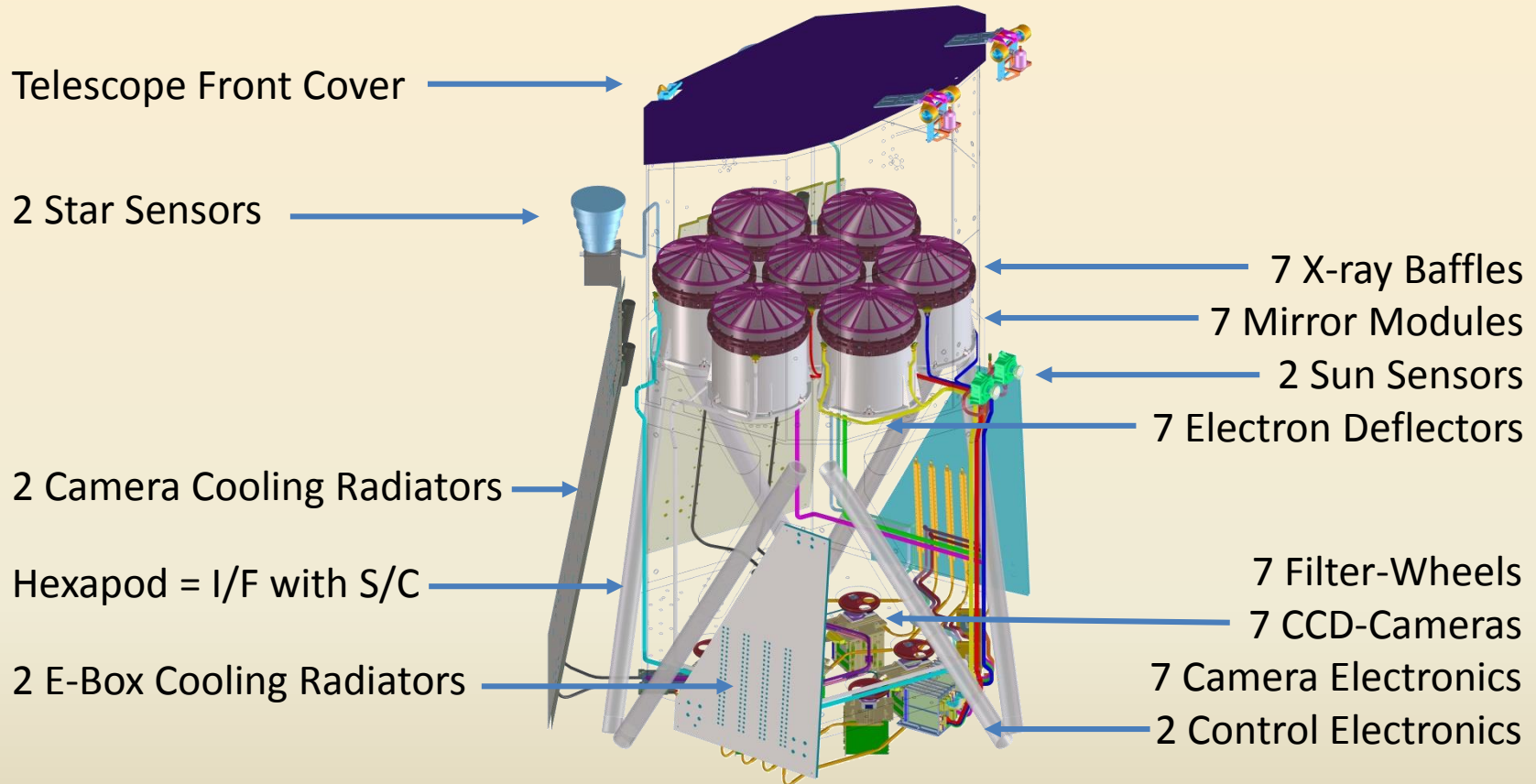
Scan of the whole sky from L2
like PLANCK, but in X-Rays,
during 4 years



eRosita is an instrument designed to perform all sky 0.5 – 10 KeV surveys: Large Field of View,

large effective area
good resolution 15-25"

Instrument

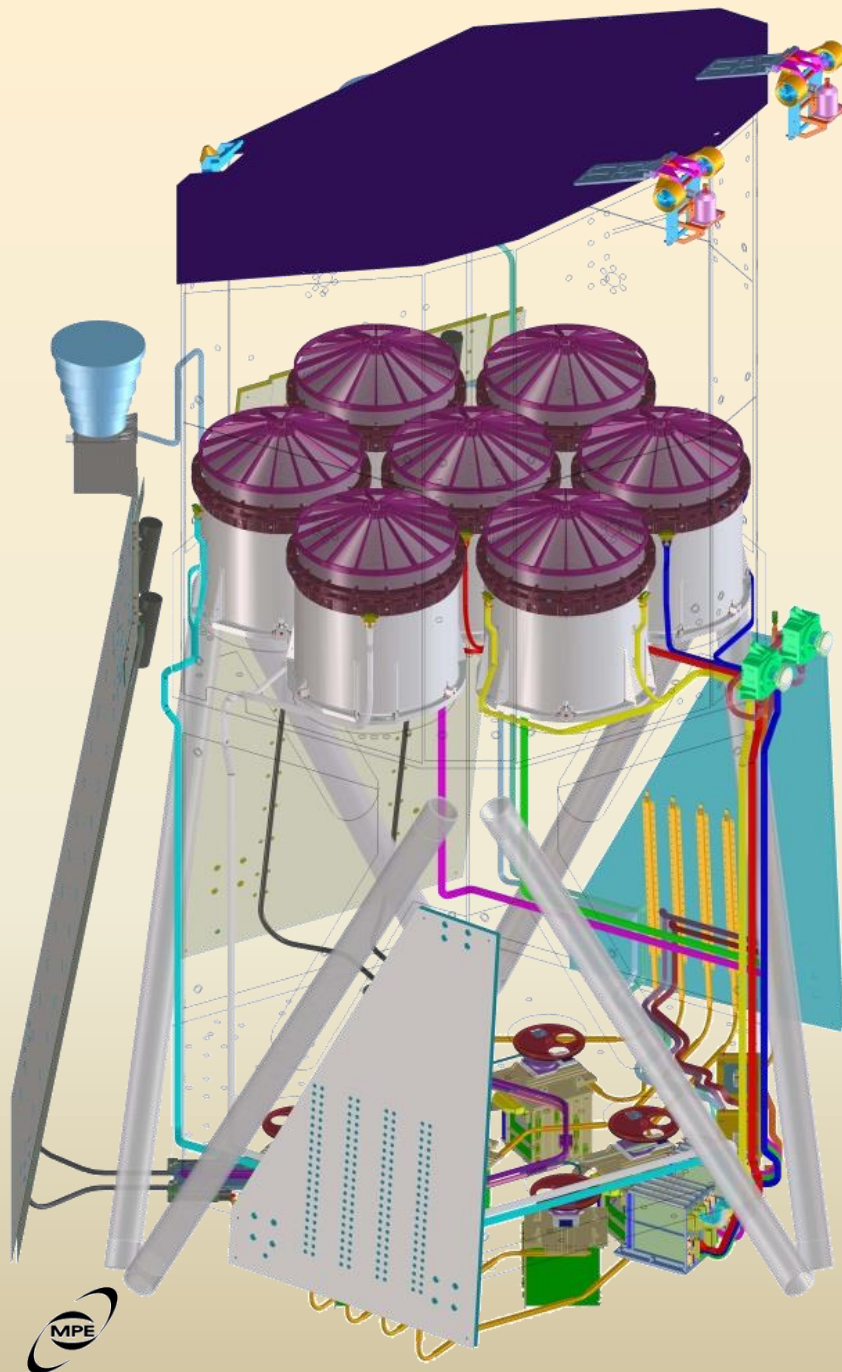


7 identical Mirror Modules
54 nested Mirror Shells each
7 identical pnCCD Cameras

Field of View
Angular Resolution
Energy Range

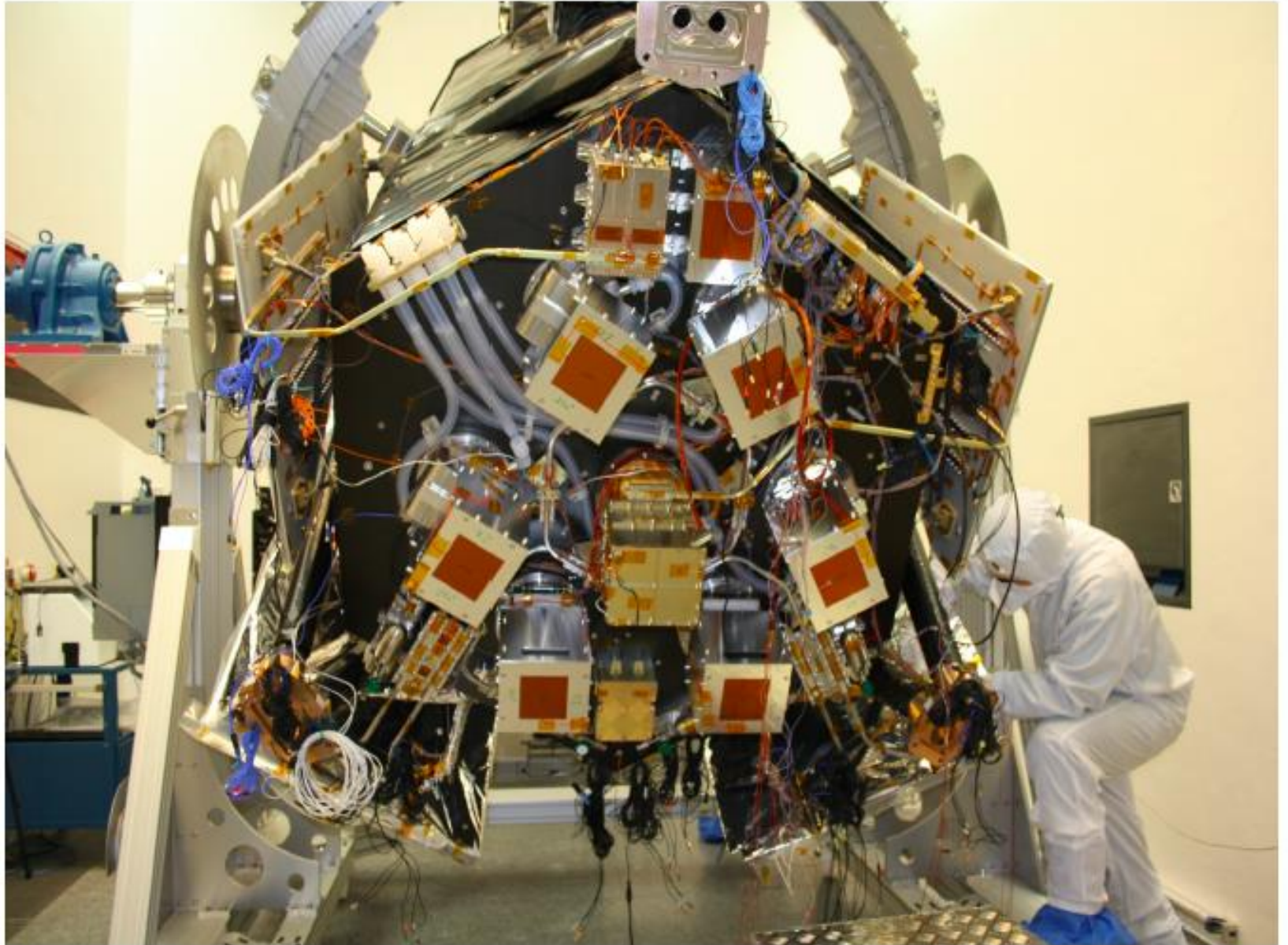
1° Ø
15 arcsec on-axis
~0,3 - 10 keV





Focal length - 1.6 m
Weight ~ 800 kg

Focal plane complexity



AGN

3 Mio. AGN

- Accretion History:
- LSS:
- AGN host Galaxies:
- Sub-Populations:
 - High Redshift ($z > 6$)
 - Extreme Luminosity
 - Compton thick AGN
- Spectra:
- Variability:
- BAOs

XLF, obscured vs. unobscured

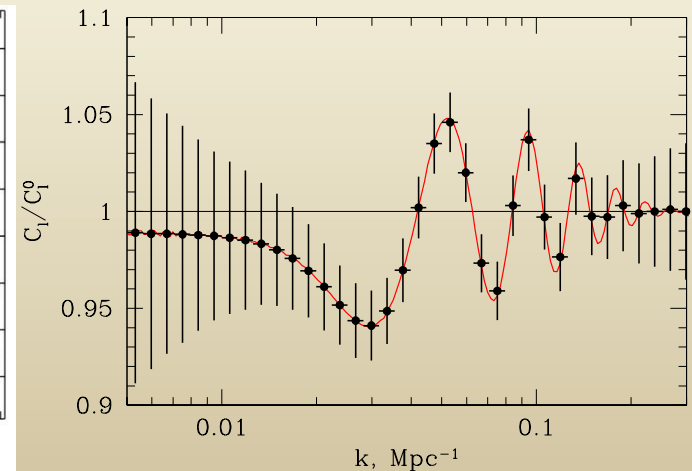
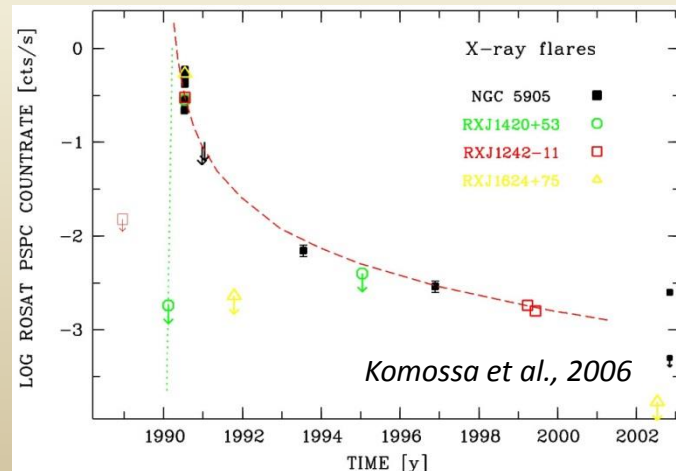
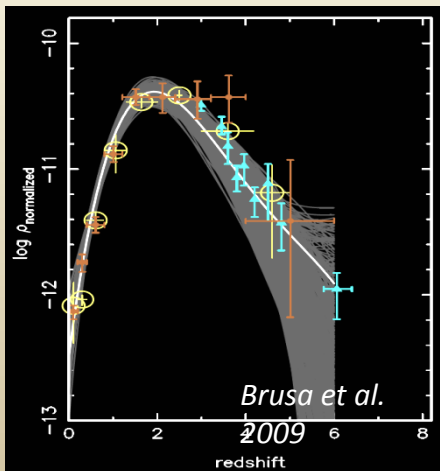
AGN ACF, AGN/Galaxy CCF, AGN/Cluster CCF

Morphology, SFR, Obscuration

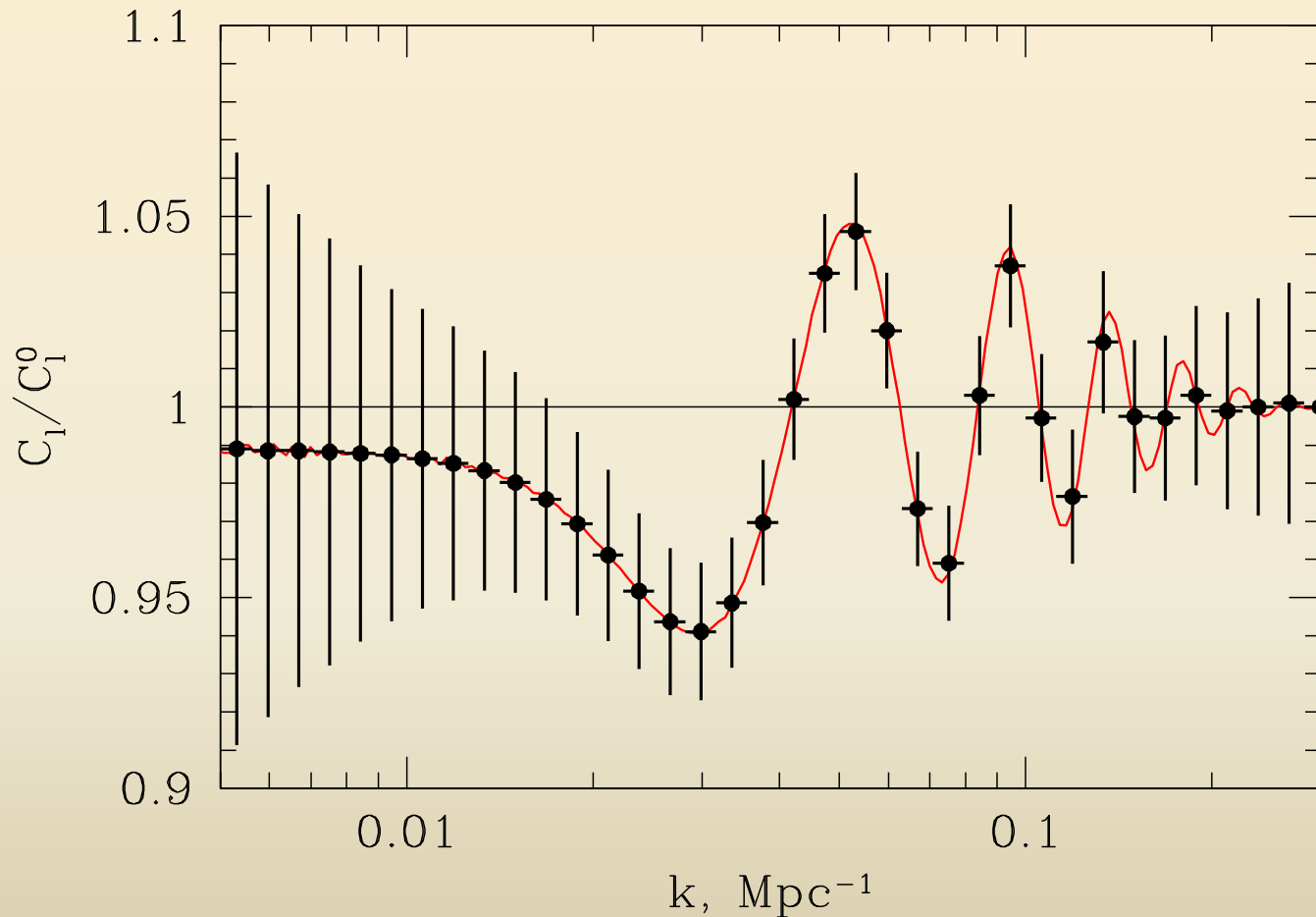
Obscuration, Continuum, Soft Excess, Iron Lines

Var. vs. L , L/L_{edd} , z , Tidal Disruptions

10σ detection, but precise redshifts needed.



AGN Cosmology: BAO



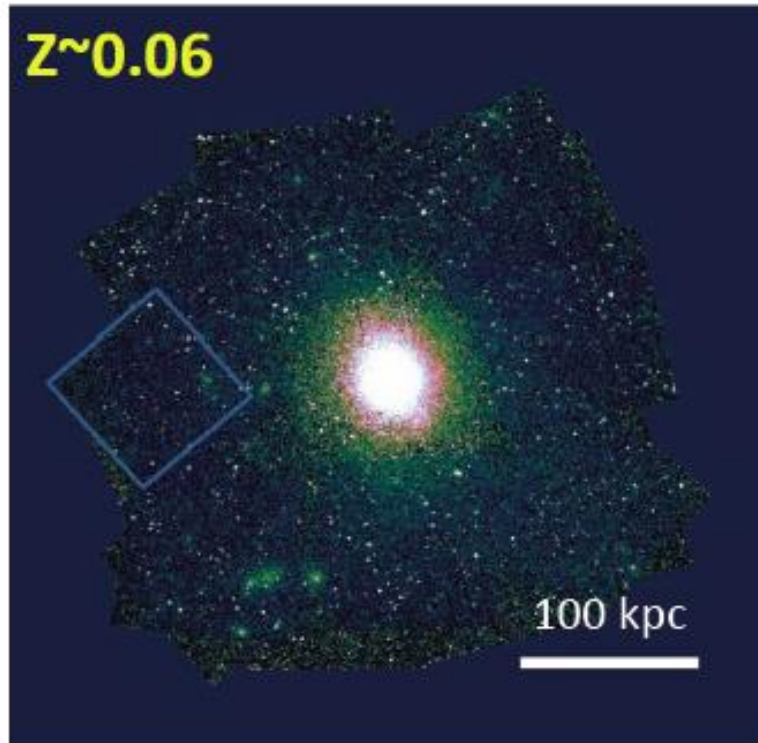
$\sim 10\sigma$
detection
using full sky
data

$\Delta z \sim 0.05$
or better is
required

A fast survey machine

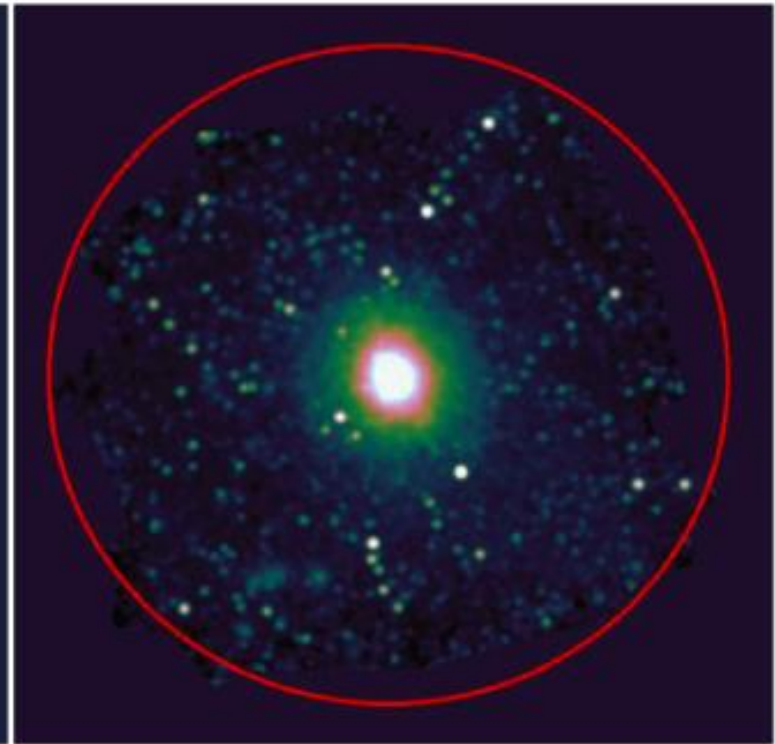
for clusters of galaxies

Chandra



~30 pointings
~2 Msec
[0.5" HEW]

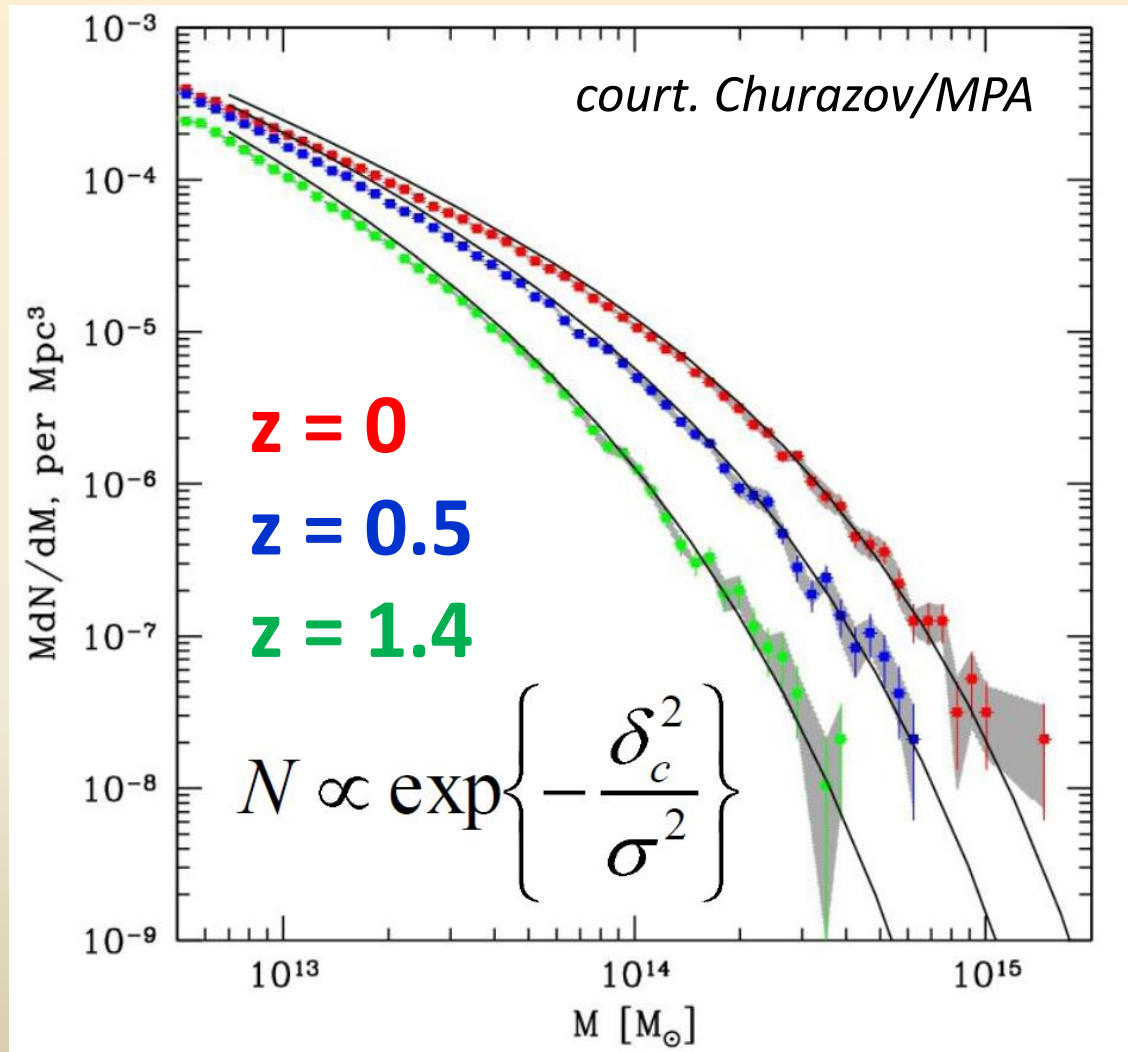
eRosita



~1 pointing
~80 ksec
[28" HEW (FoV avg)]

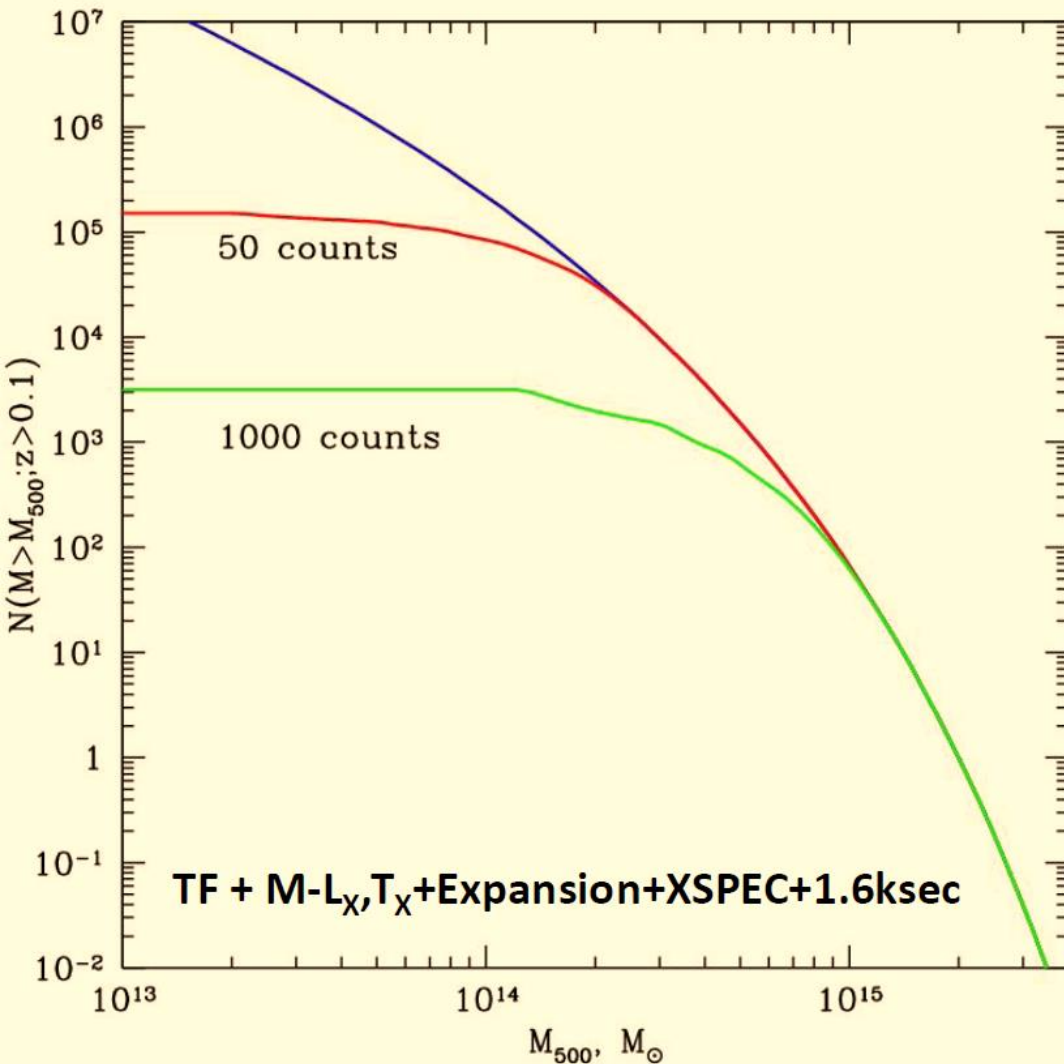
Churazov, IKI, MPA

Evolution of Cluster Mass Function



Number of most massive clusters is extremely sensitive to cosmology

Will eROSITA detect all Clusters?



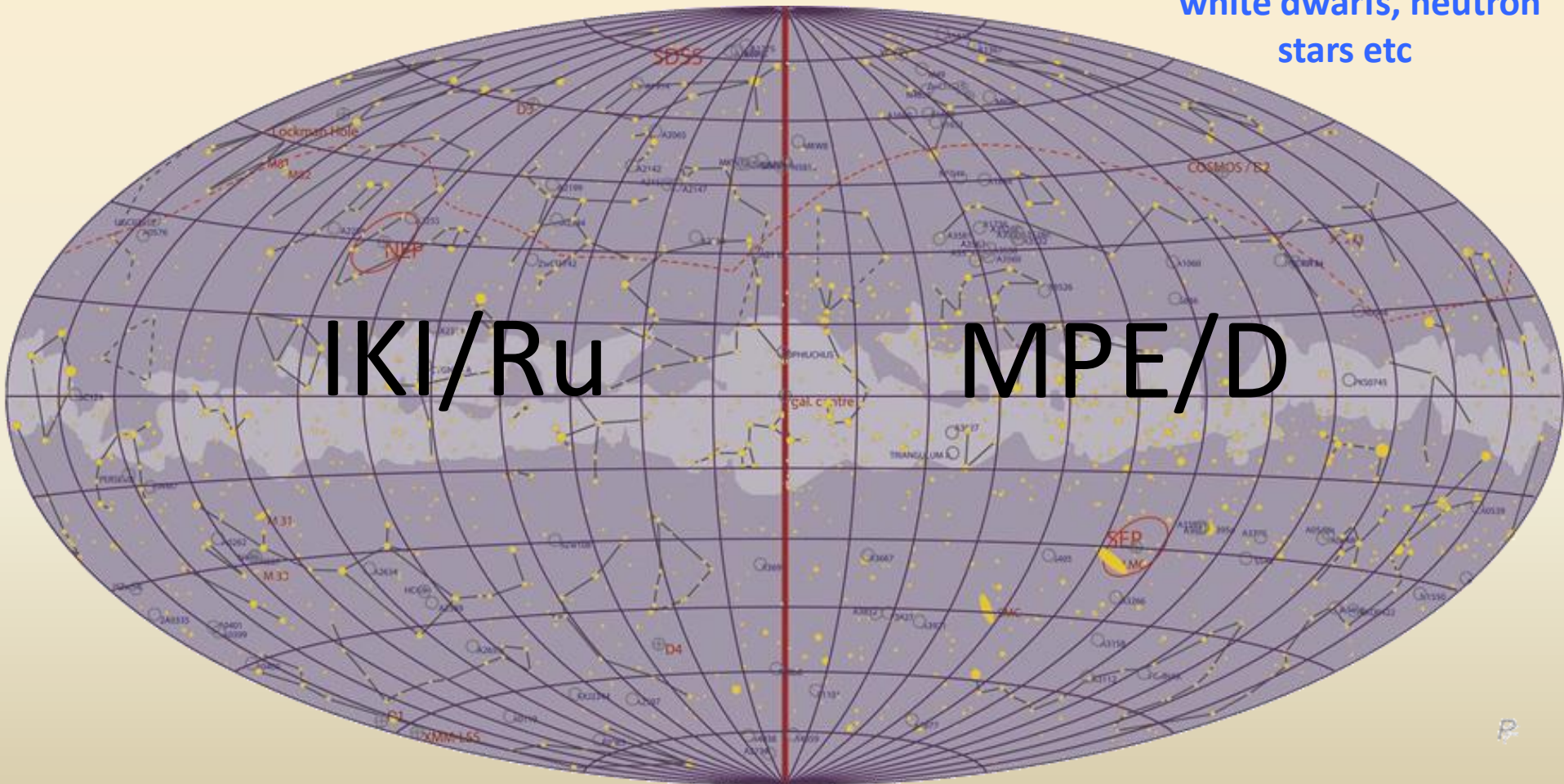
M	z	N	eRosita
10^{14}	~ 3	$8 \cdot 10^4$	40%
$3 \cdot 10^{14}$	~ 2	$8 \cdot 10^3$	100%
10^{15}	~ 1	50	100%

Churazov/IKI, MPA: Yes!

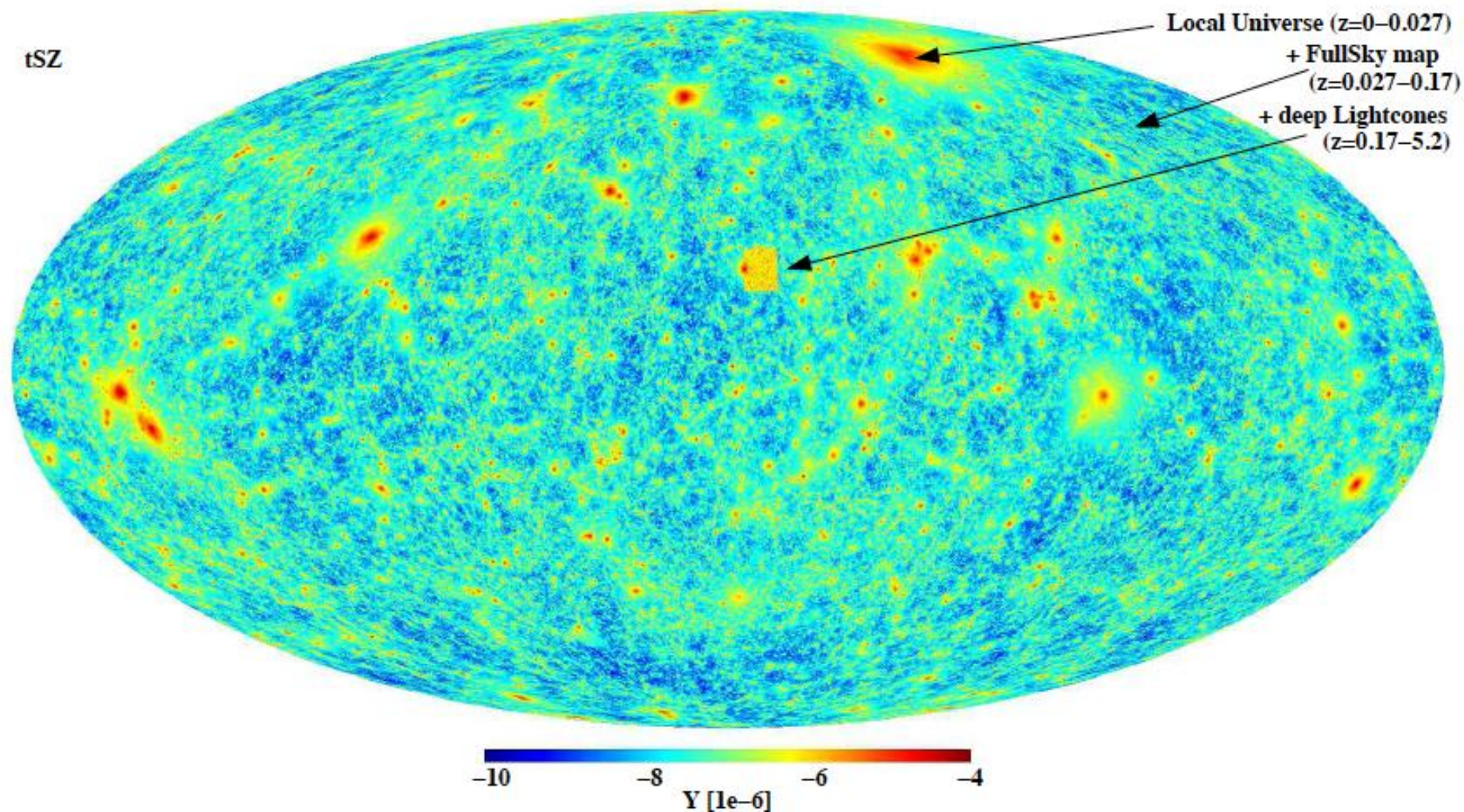
$z_{\max} \sim 2, \quad M \sim 3 \cdot 10^{14} M_{\text{Sun}}$

Sky Division

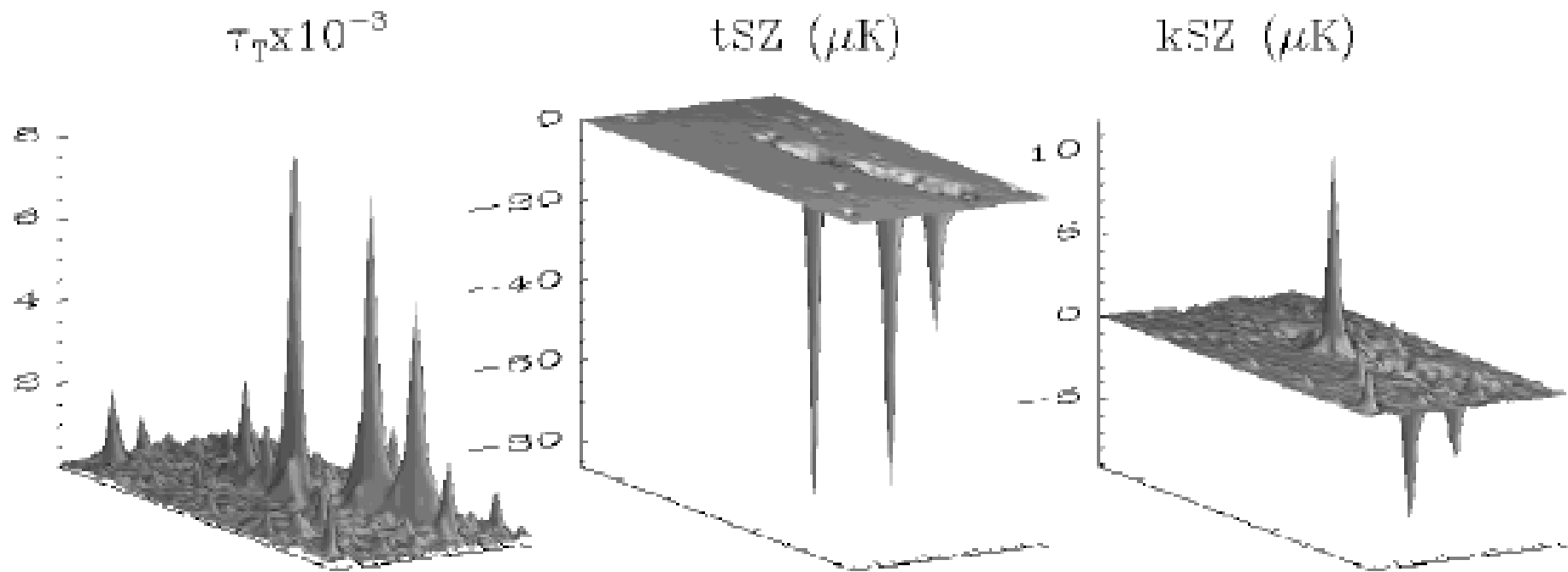
**Hundreds of thousands
Galactic X-Ray sources:**
supernovae remnants,
young stars and stars
with active coronae,
white dwarfs, neutron
stars etc



tSZ



It will be great to overlap eRosita map with 100 000 clusters and groups of galaxies
onto high quality y-map from the future CMB spacecraft



Diarerio, Sunyaev, Nusser, 2003

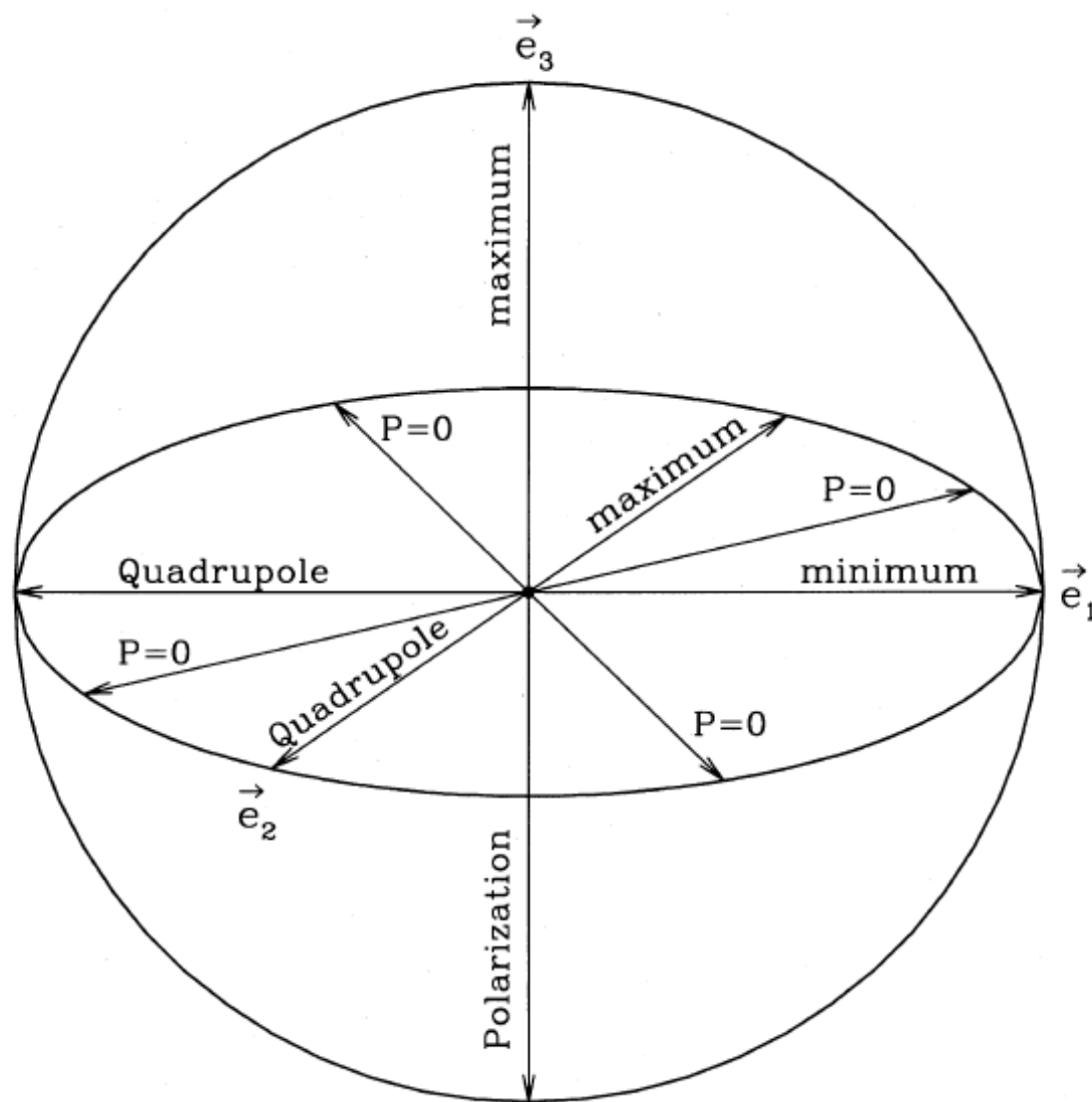


Figure 1. The geometry of the polarization effect induced by the CMB quadrupole. The vectors \vec{e}_1 , \vec{e}_2 and \vec{e}_3 define the eigensystem of the CMB quadrupole temperature anisotropy. The polarization effect has two broad maxima in the directions $\pm\vec{e}_3$ orthogonal to the plane which contains the minima ($\pm\vec{e}_1$) and maxima ($\pm\vec{e}_2$) of the quadrupole. In the same plane there are four directions for which there is no polarization.

Archaeology with polarisation in clusters of galaxies

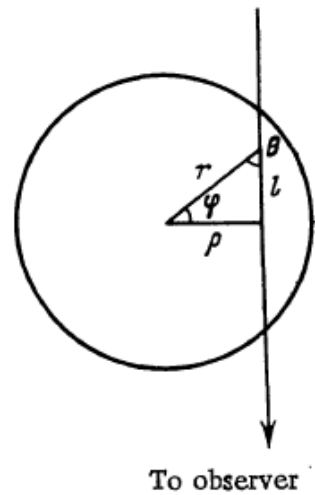


FIG. 1. Geometry of the problem of the scattering of the radio waves emitted by a central source in a cluster of galaxies.

Quasars are variable,
we can see the history
of their activity in the
reflected radiowaves
(traces of the jets)

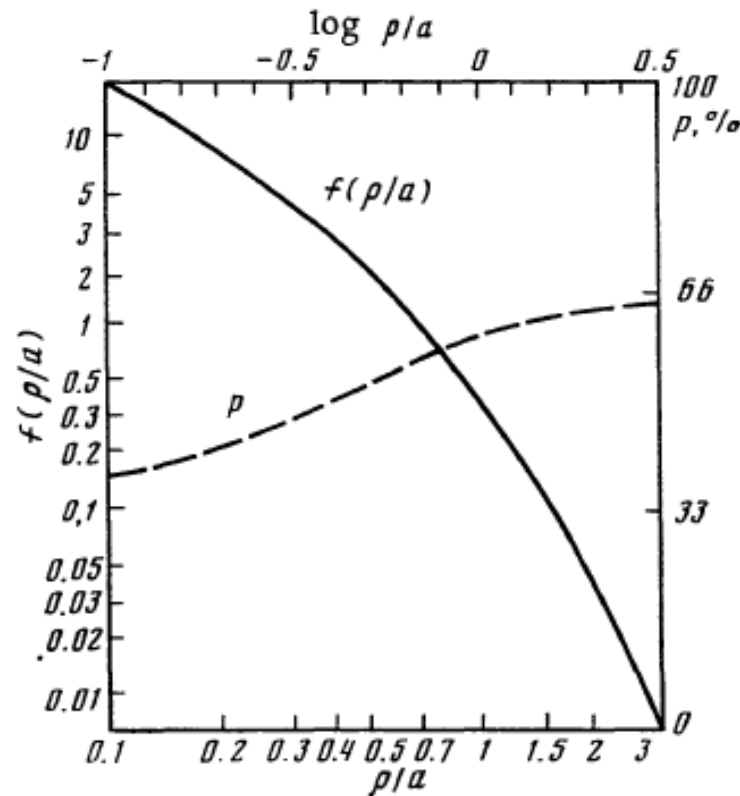


FIG. 2. Solid curve, the function $f(\rho/a)$ describing the dependence of the diffuse scattered radiation intensity on the distance of the line of sight from the compact radio source at the center of a galaxy cluster of core radius a . Dashed curve, percentage polarization of the diffuse radiation as a function of ρ/a .

Thank you !!!

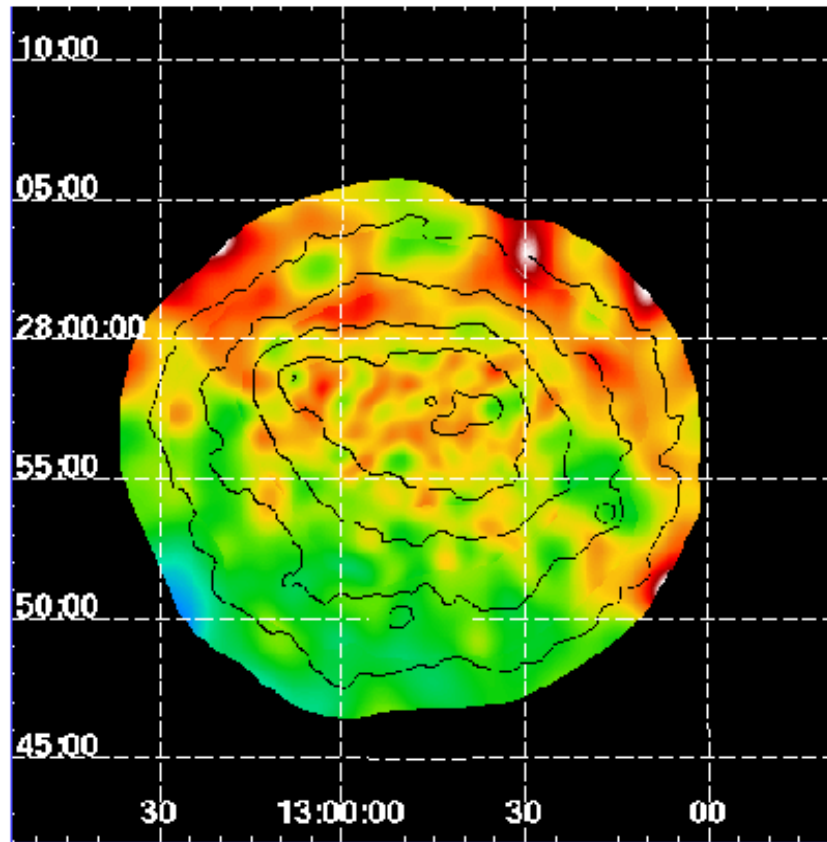




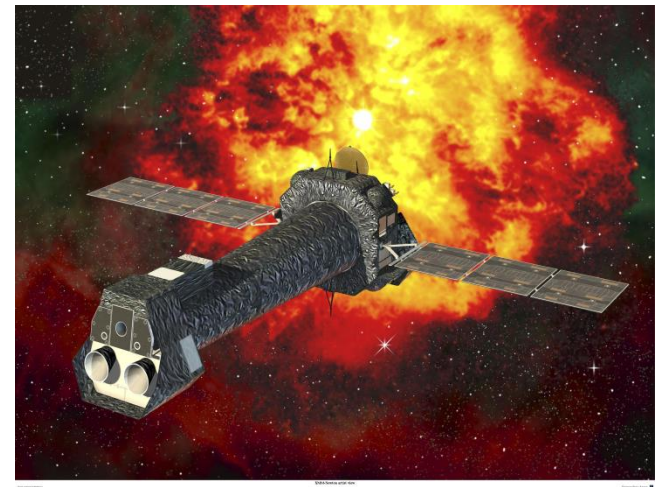
Bose-Einstein spectrum

$$\begin{aligned}n_{\text{BE}} &= \frac{1}{e^{\frac{h\nu}{k_{\text{B}}T_{\text{BE}}} + \mu} - 1} \\&= \frac{1}{e^{x-0.456\mu x + \mu} - 1} \\&\approx n_{\text{pl}}(x) + \frac{\mu e^x}{(e^x - 1)^2} \left(\frac{x}{2.19} - 1 \right),\end{aligned}$$

X-RAY EMISSION FROM CLUSTERS OF GALAXIES



COMA CLUSTER TEMPERATURE MAP (XMM-Newton)
(Briel et al. 2001, image by Churazov)



Electron temperature ~ 9 KeV

Electron density $\sim 0.03 \text{ cm}^{-3}$

Dark matter mass –
up to $10^{15} M_{\text{sun}}$

$M_{\text{sun}} = 2 \cdot 10^{33} \text{ g}$

Sound velocity of gas is close to velocities of galaxies

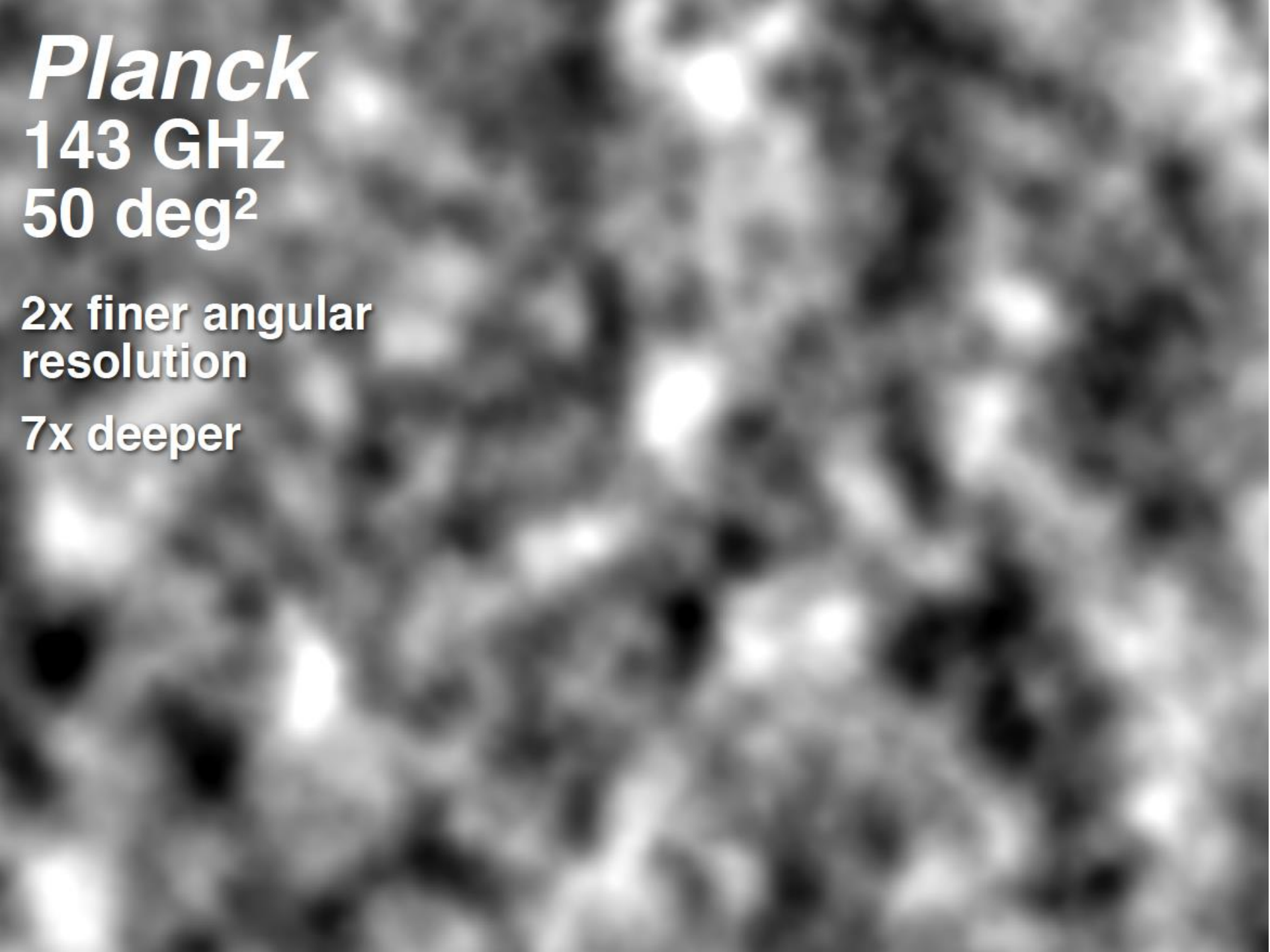
Planck

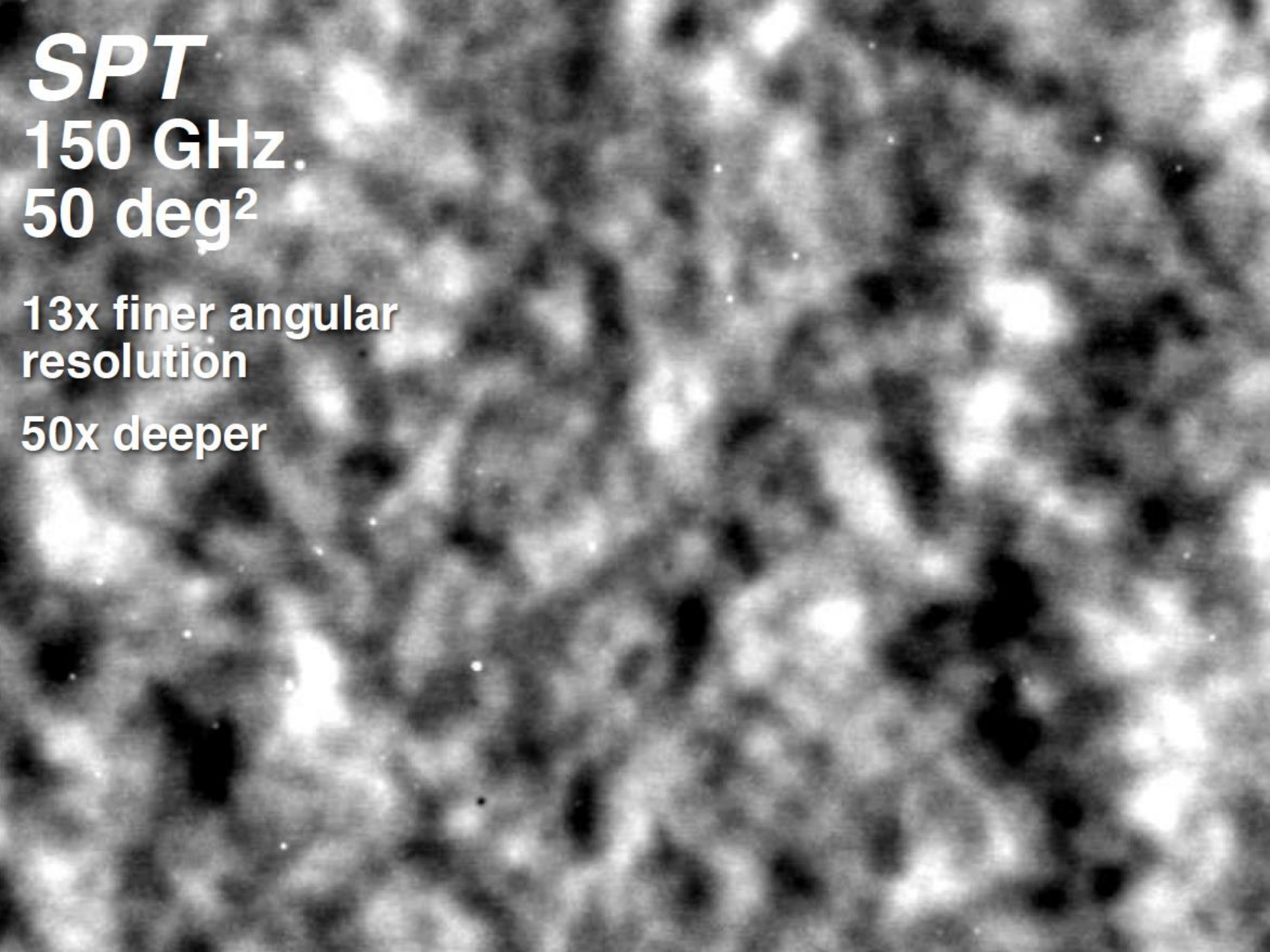
143 GHz

50 deg²

**2x finer angular
resolution**

7x deeper





SPT

150 GHz.

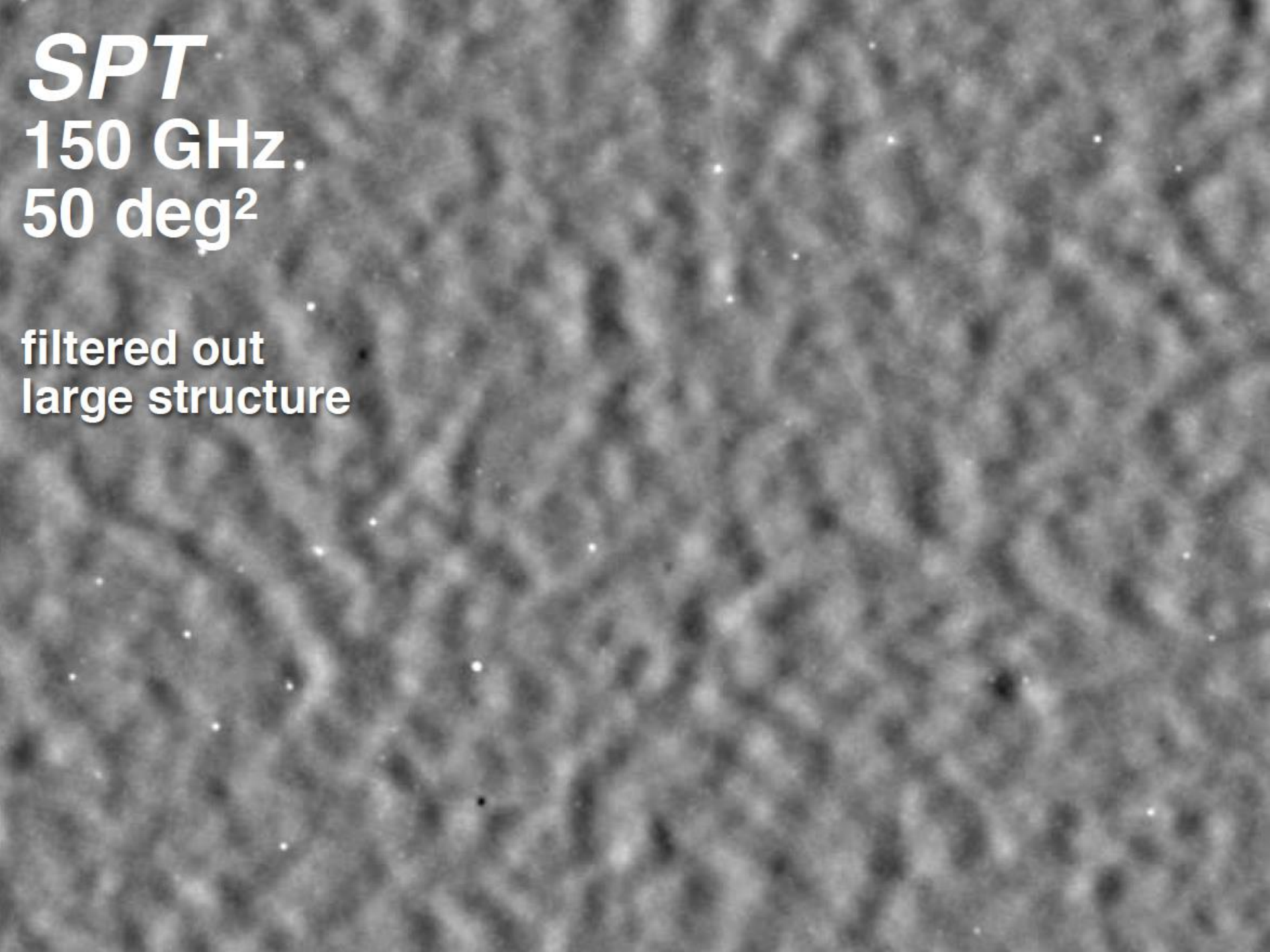
50 deg²

**13x finer angular
resolution**

50x deeper

SPT
150 GHz.
50 deg²

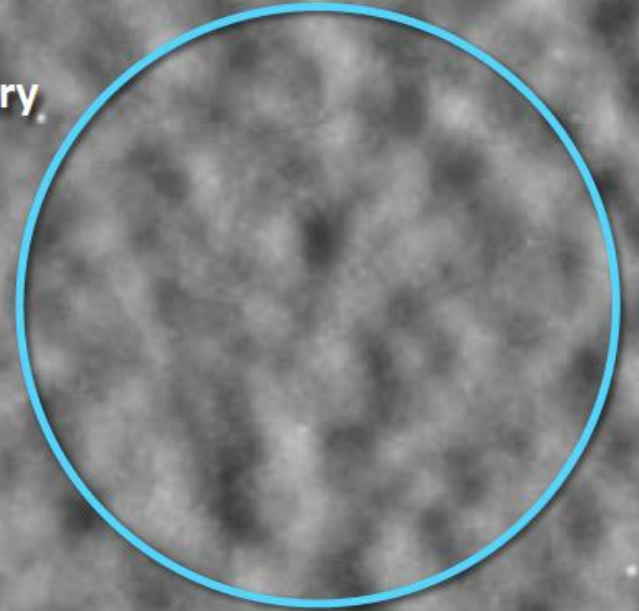
**filtered out
large structure**



SPT
150 GHz.
50 deg²

CMB Anisotropy

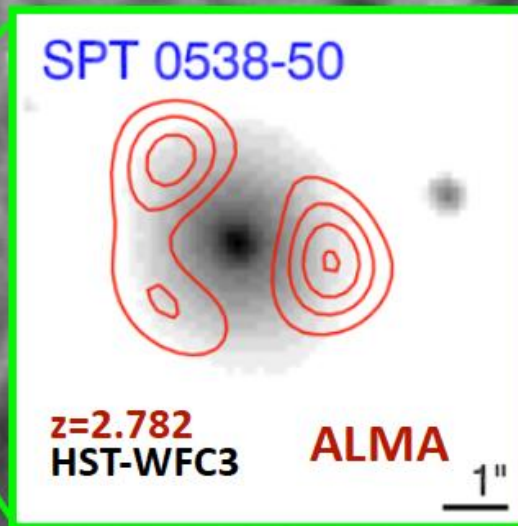
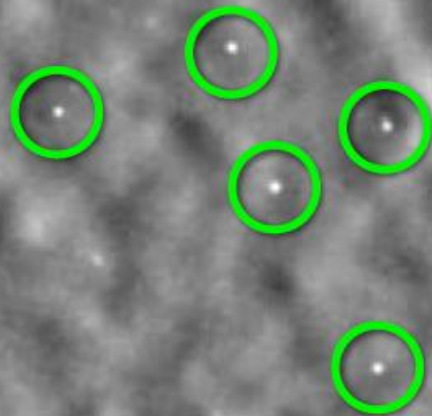
Primordial and secondary
anisotropy in the CMB



SPT
150 GHz.
50 deg²

Point Sources

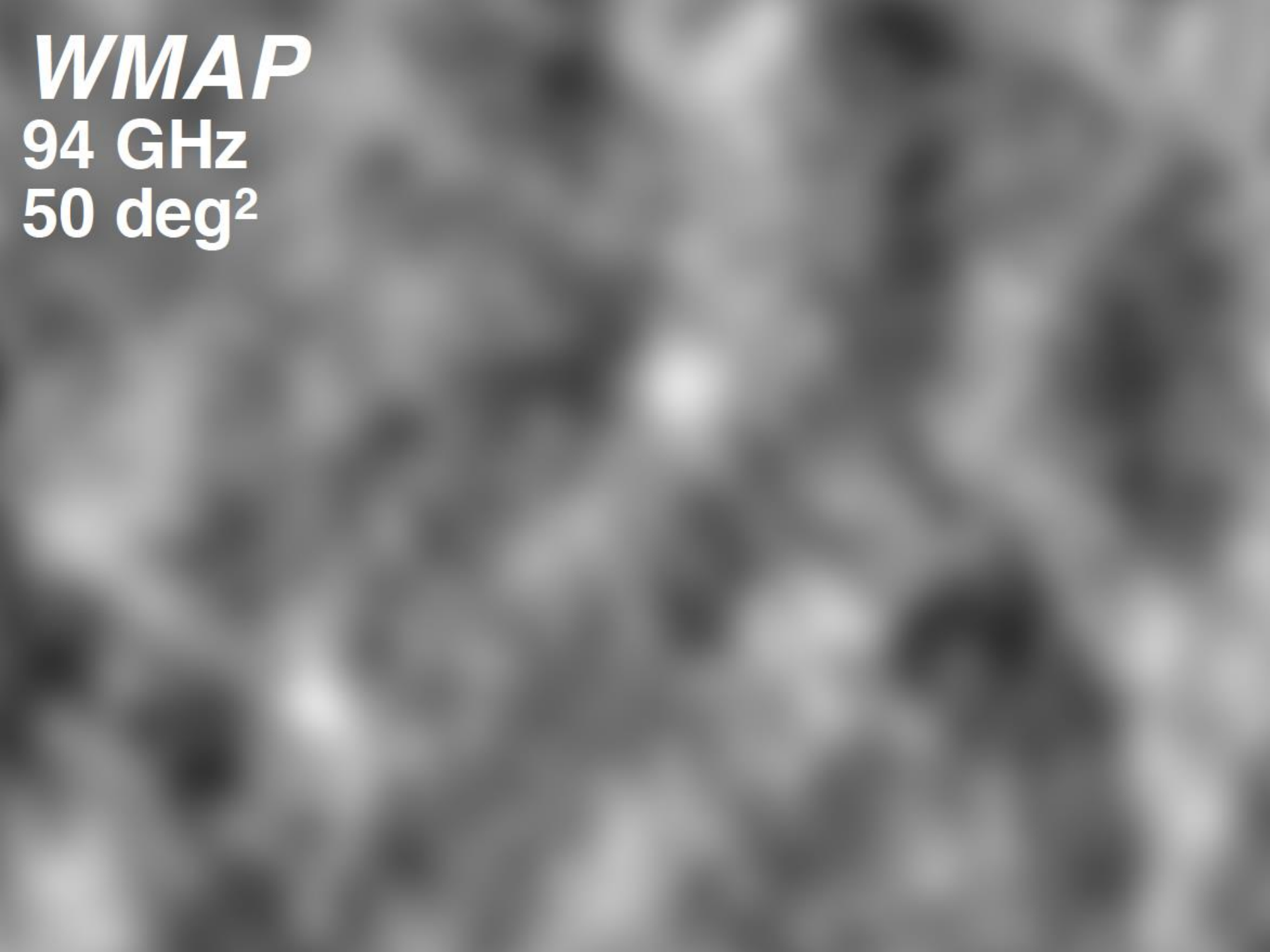
Active galactic nuclei, and the most
distant, star-forming galaxies



WMAP

94 GHz

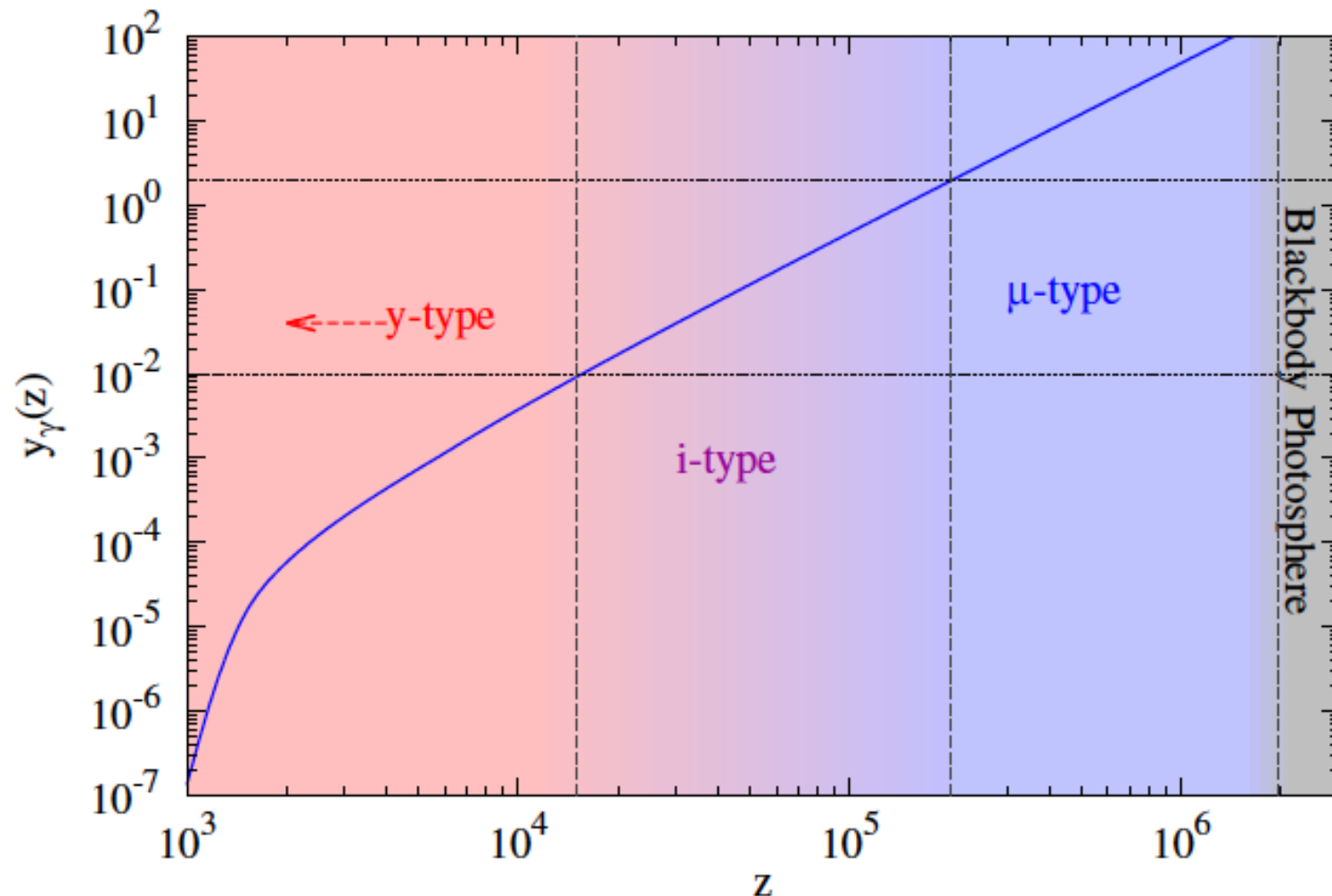
50 deg²



For $y_\gamma \gg 1$ equilibrium is established.

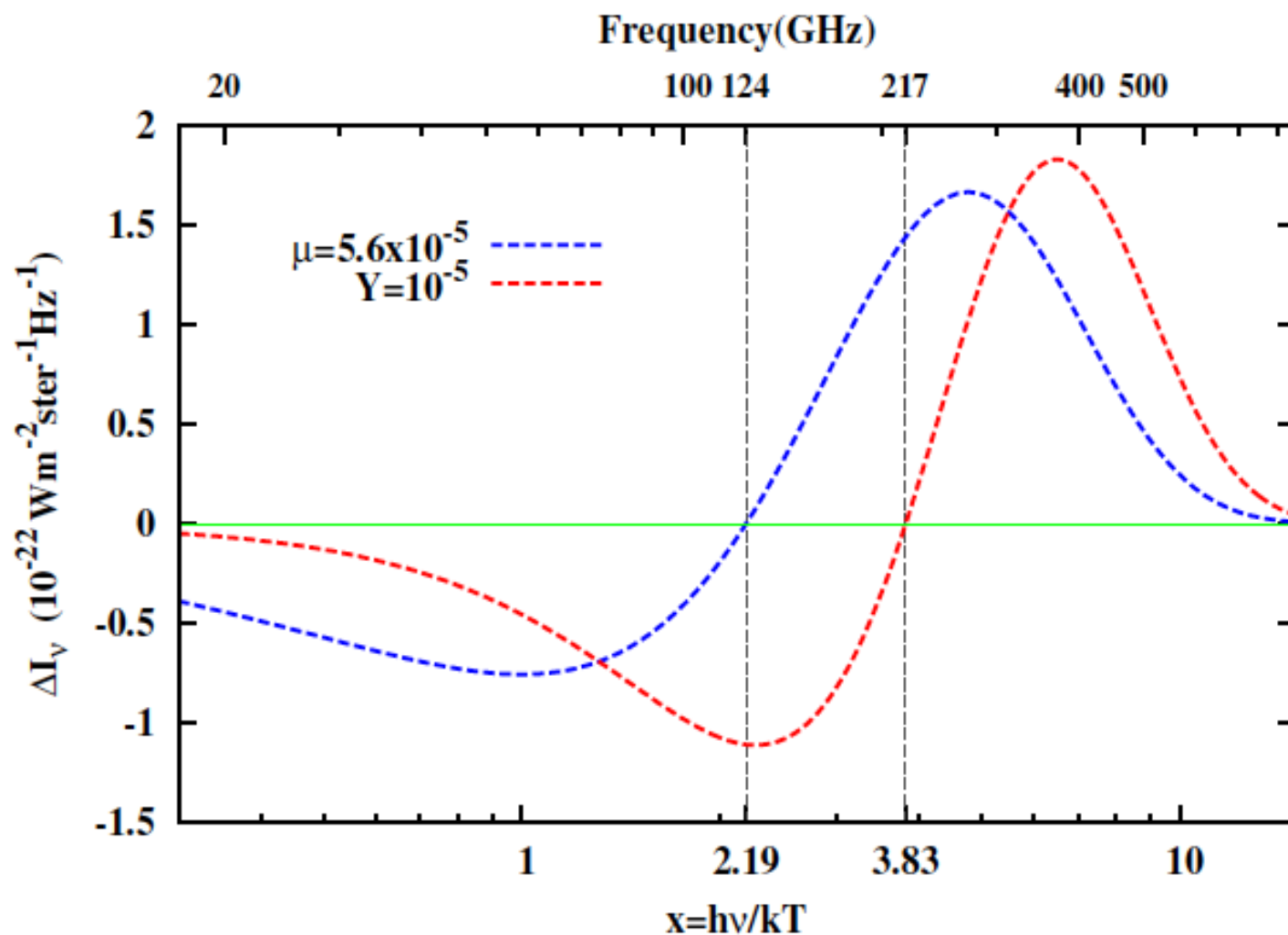
T_e and T_γ converge to common value

The photon spectrum relaxes to equilibrium Bose-Einstein distribution

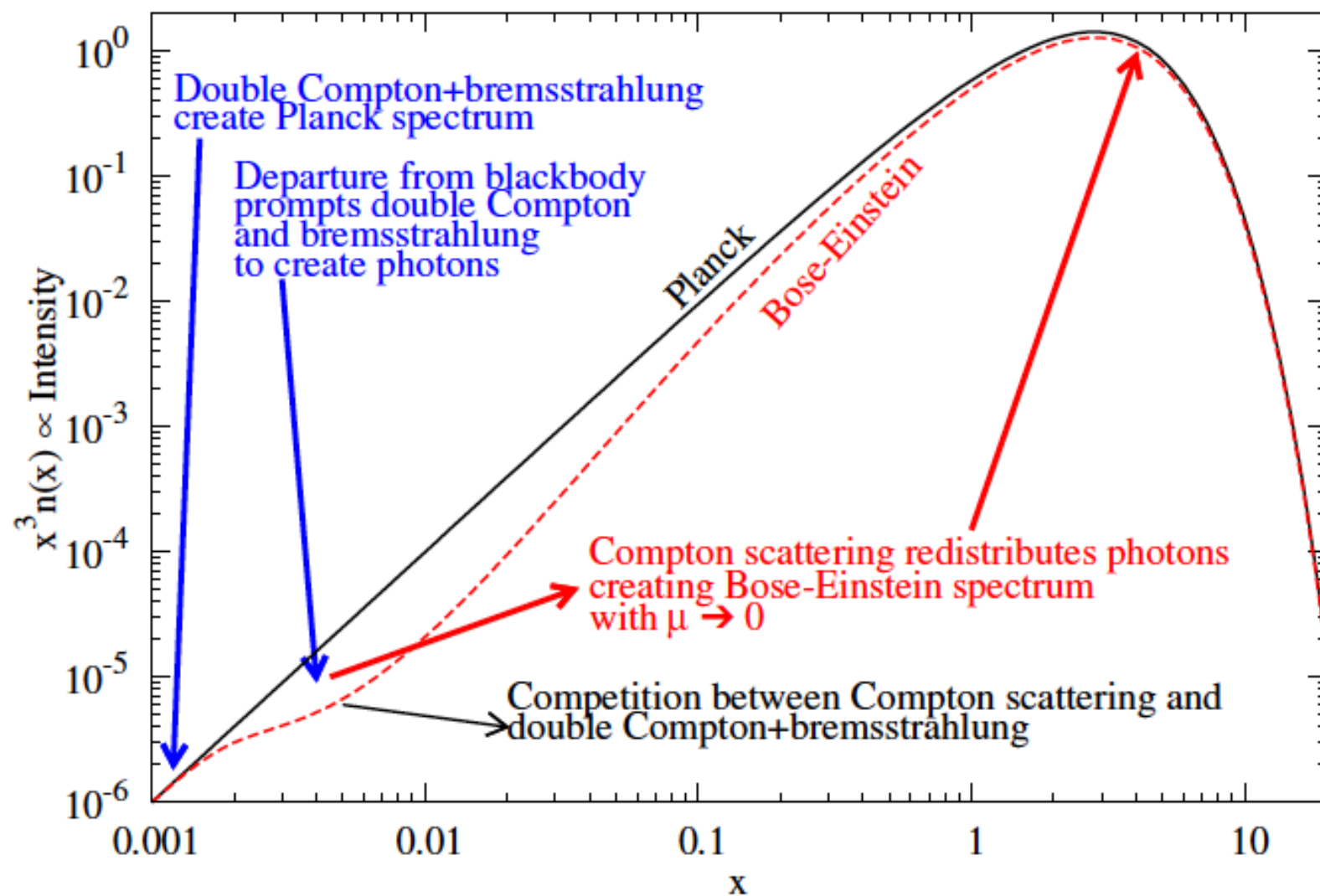


μ -distortion: Bose-Einstein spectrum, $y_\gamma \gg 1$

COBE-FIRAS limit (95%): $\mu \lesssim 9 \times 10^{-5}$ (Fixsen et al. 1996)



Creation of CMB Planck spectrum



Analytical solution (Sunyaev, Zeldovich, 1970)

$$\mu = \mu(t_0) e^{-2 \sqrt{ak} (t - t_0)}$$

Where a and k are scattering (Comptonisation) and real absorption coefficients correspondently

In the case of Double Compton (emission of second photon during scattering) spectral deviations decrease with time

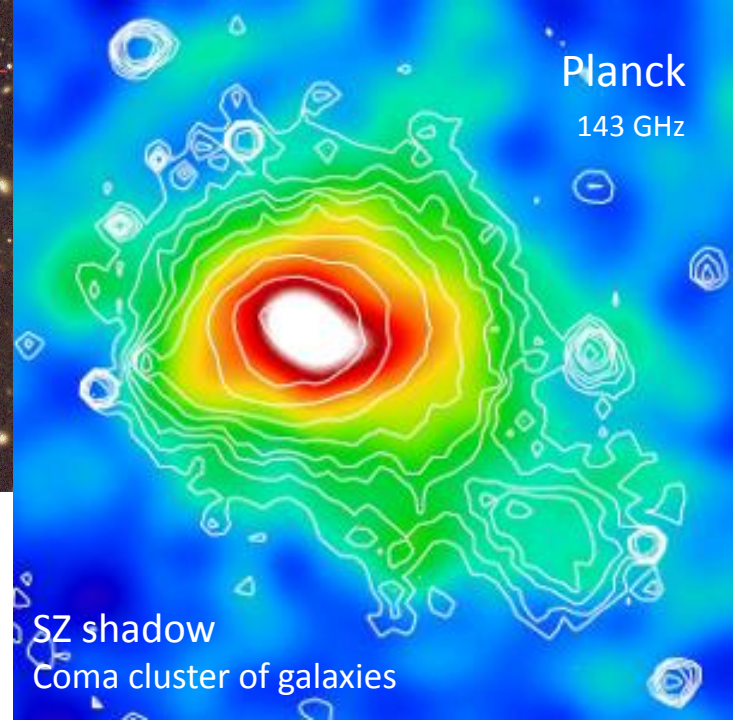
$$\frac{\mu^{\text{final}}}{\mu^{\text{initial}}} \approx e^{-(z_i/z_{\text{dc}})^{5/2}}$$

Danese, de Zotti, 1984

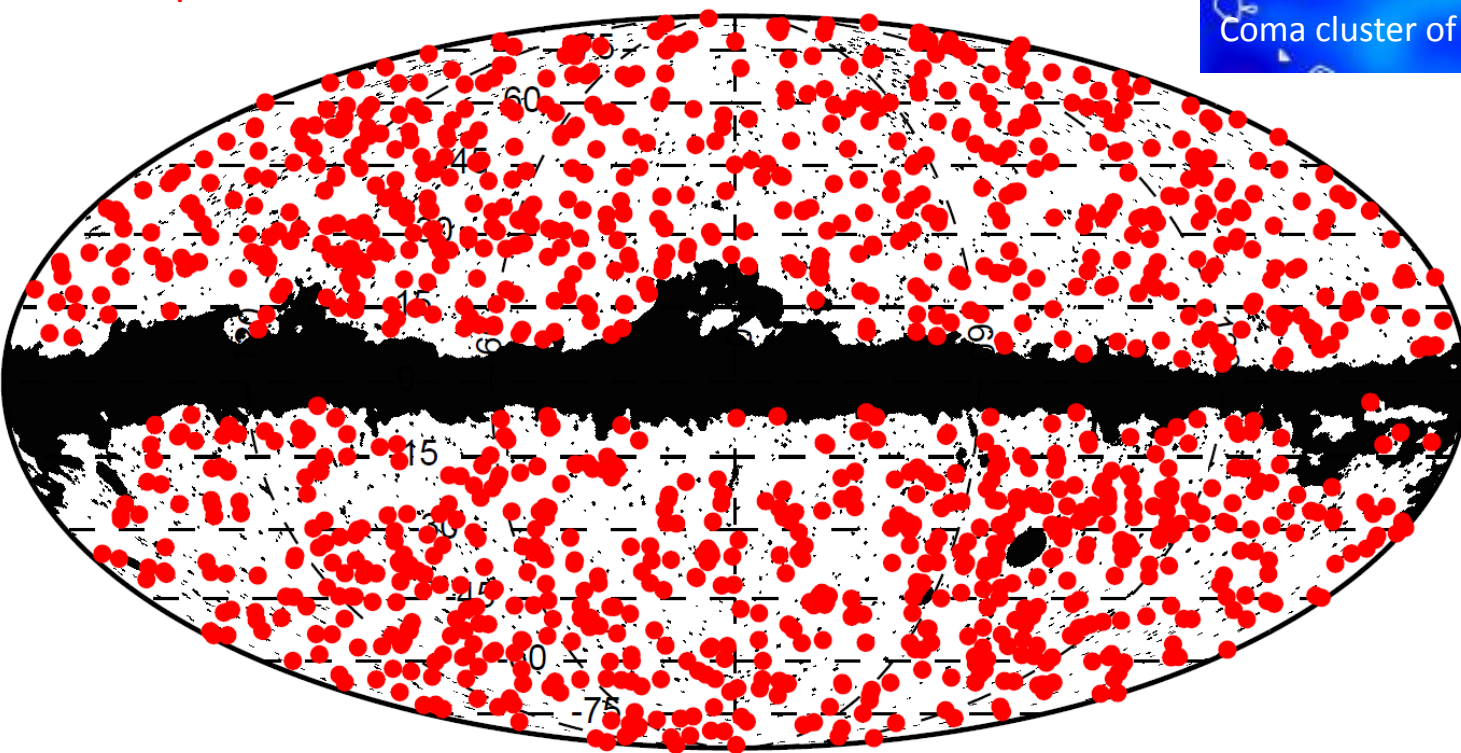
PLANCK/HFI



*Coma, optical image
central part*



~ 900 clusters confirmed by X-Ray
or optical observations

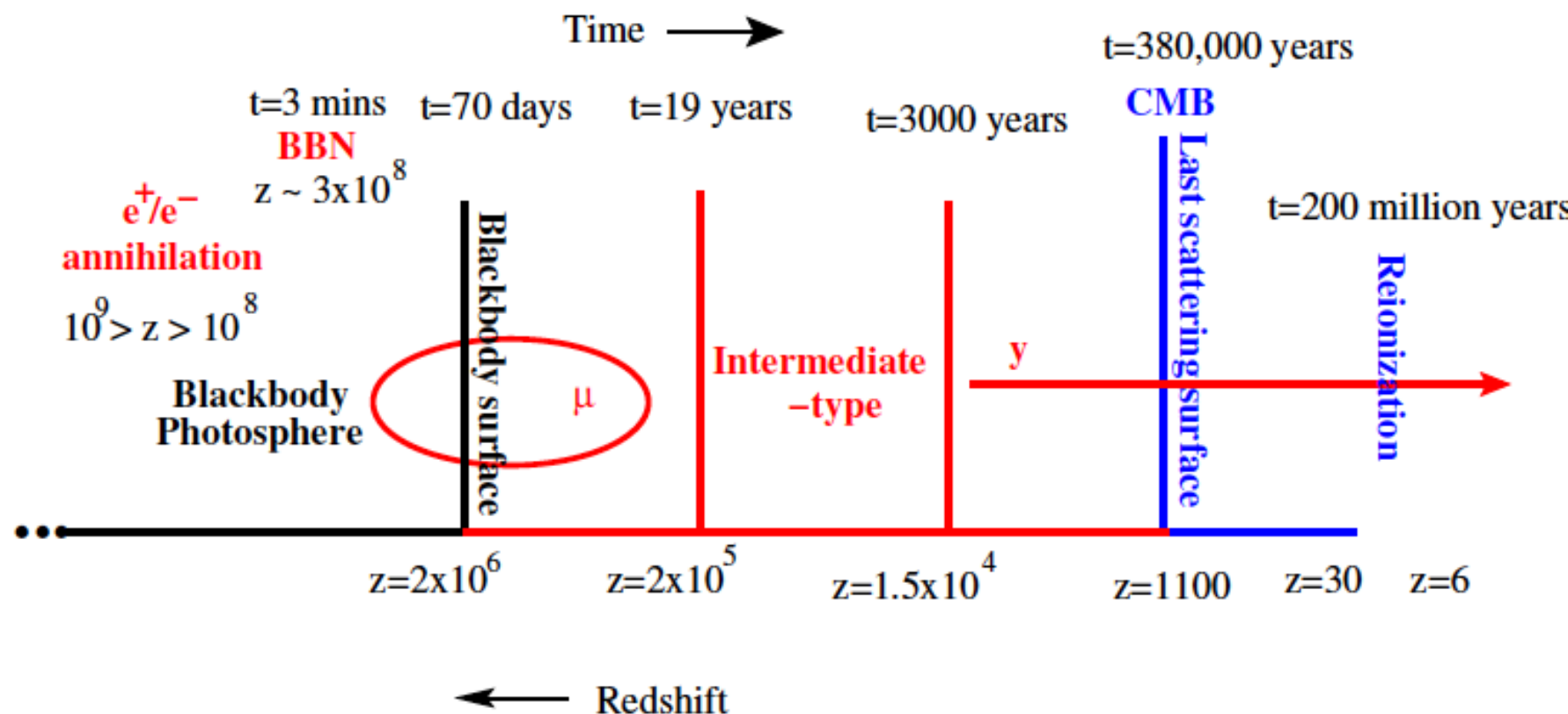


$$n_{SZ} = y \; T^4 \frac{\partial}{\partial T} \frac{1}{T^2} \frac{\partial n_{Pl}}{\partial T}$$

$$= y \; \frac{\mathbf{x} \mathbf{e}^{\mathbf{x}}}{(\mathbf{e}^{\mathbf{x}} - \mathbf{1})^2} \left(\mathbf{x} \frac{\mathbf{e}^{\mathbf{x}} + \mathbf{1}}{\mathbf{e}^{\mathbf{x}} - \mathbf{1}} - \mathbf{4} \right)$$

$$\Delta I_{sz} = I_{sz} - I_{planck} = \frac{2h\nu^3}{c^2} n_{sz}$$

μ -type distortions

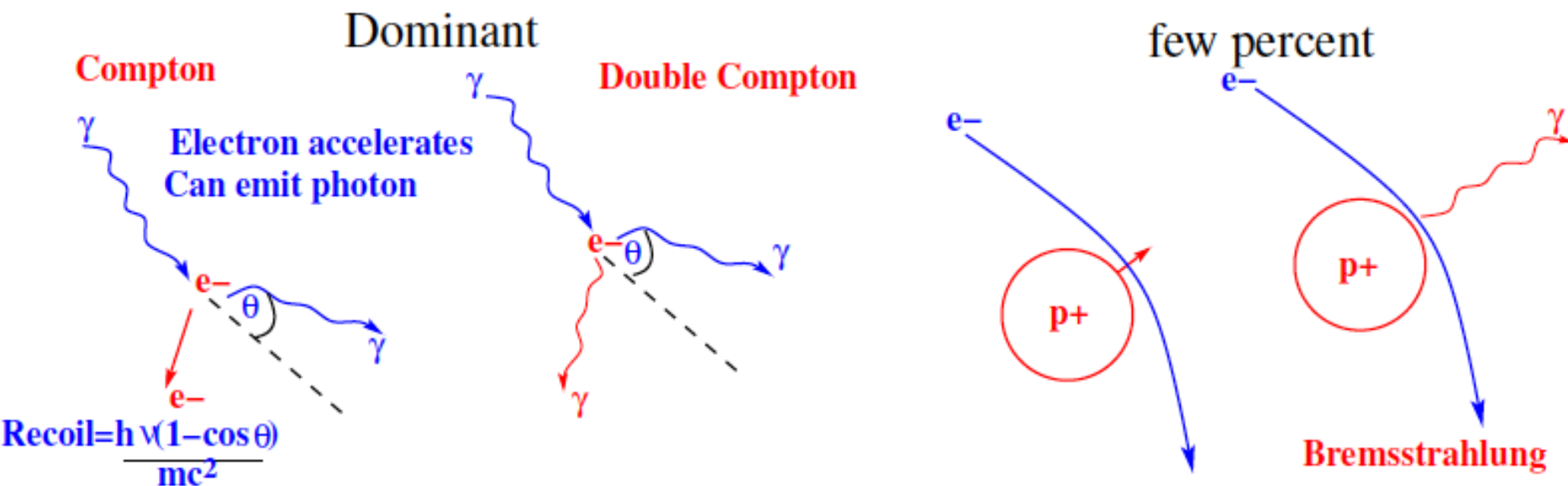


Compton + double Compton + bremsstrahlung

Analytic solution: $\mu = 1.4 \int \frac{dQ}{dz} e^{-\mathcal{T}(z)} dz$

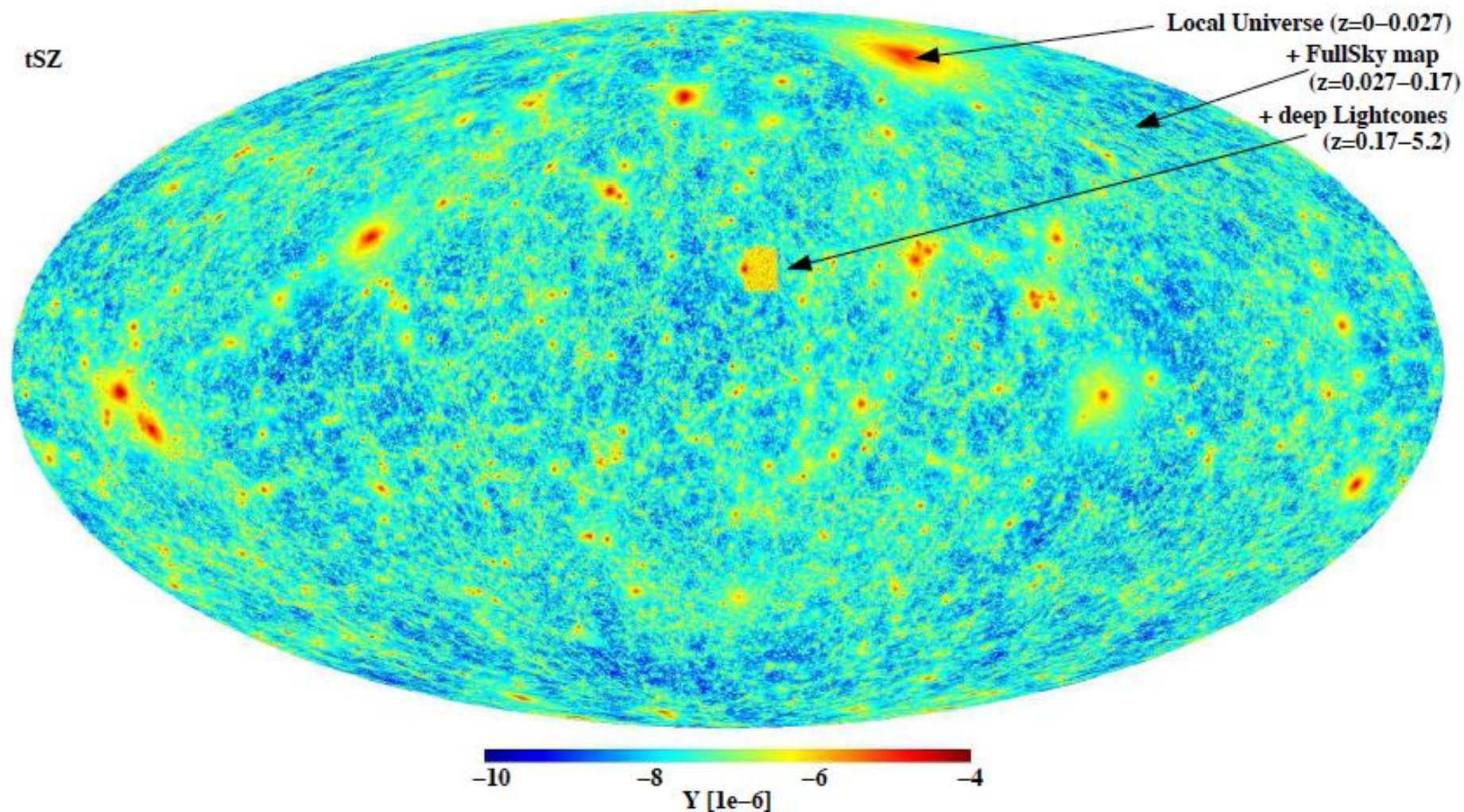
(Sunyaev and Zeldovich 1970)

Processes responsible for creation of CMB spectrum



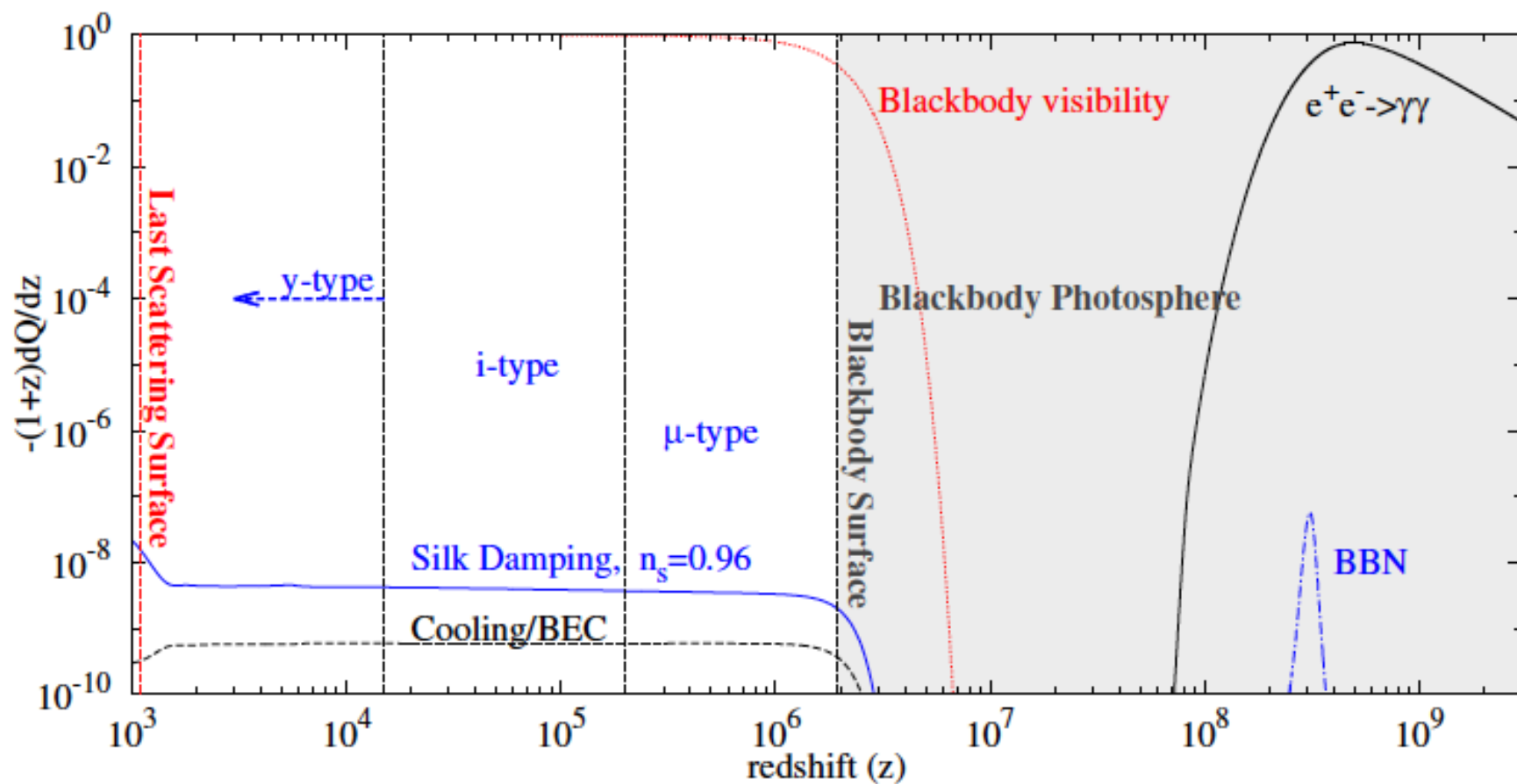
- ▶ Double Compton and bremsstrahlung create/absorb photons ($\propto 1/x^2$)
- ▶ Compton scattering distributes them over the whole spectrum

tSZ



It will be great to overlap eRosita map with 100 000 clusters and groups of galaxies
onto high quality y-map from the future CMB spacecraft

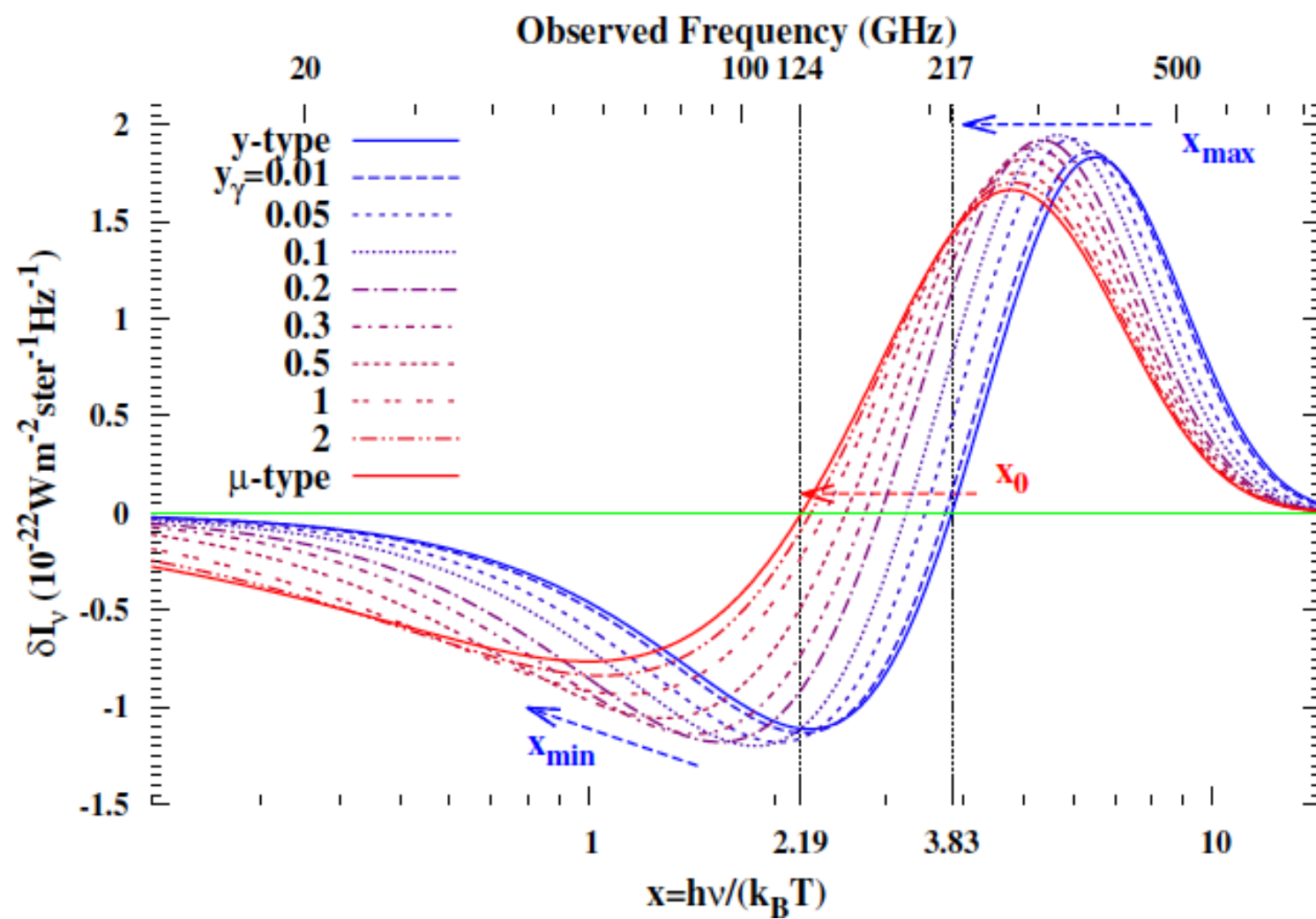
The general picture



Intermediate-type distortions (*Khatri and Sunyaev 2012b*)

Solve Kompaneets equation with initial condition of y-type solution.

$$\frac{\partial n}{\partial y_\gamma} = \frac{1}{x^2} \frac{\partial}{\partial x} x^4 \left(n + n^2 + \frac{T_e}{T} \frac{\partial n}{\partial x} \right), \quad \frac{T_e}{T} = \frac{\int (n + n^2) x^4 dx}{4 \int n x^3 dx}$$



Bose-Einstein spectrum- Chemical potential (μ)

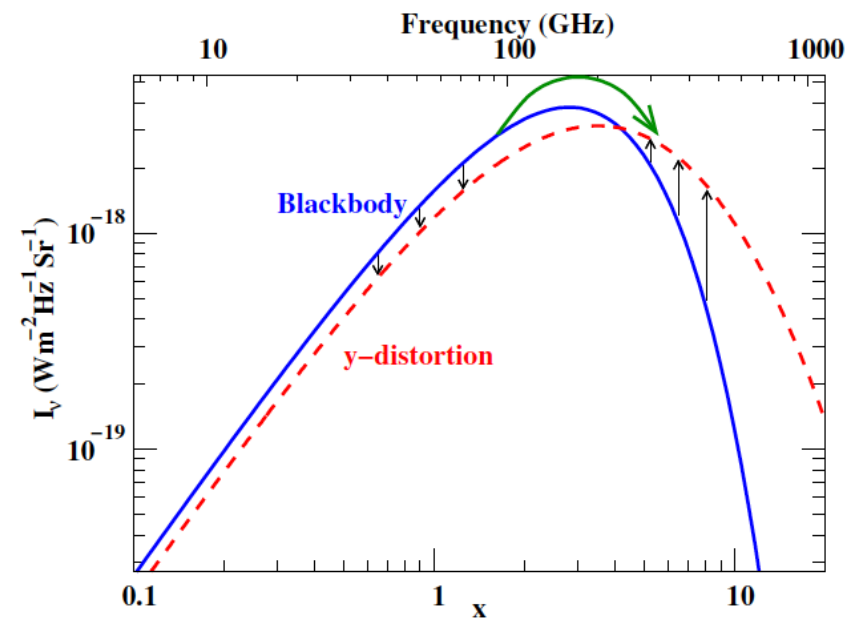
$$n(x) = \frac{1}{e^{x+\mu} - 1}$$

Given two constraints, energy density (E) and number density (N) of photons, T, μ uniquely determined.

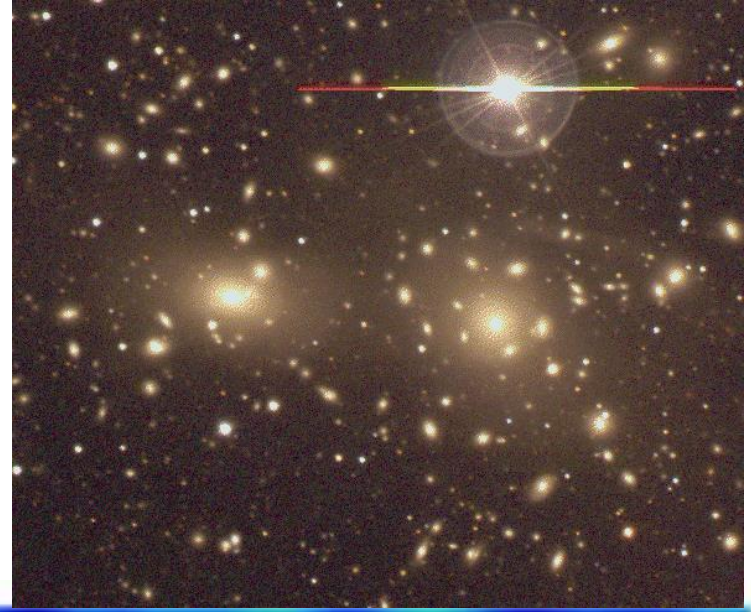
Idea behind analytic solutions:

If we know rate of production of photons and energy injection rate, we can calculate the evolution/production of μ (and T)

(Zeldovich and Sunyaev 1969)
 COBE-FIRAS limit (95%): $y \lesssim 1.5 \times 10^{-5}$ (Fixsen et al. 1996)



Coma,
 optical
 image,
 central
 part



$$n_{SZ} = y \, T^4 \frac{\partial}{\partial T} \frac{1}{T^2} \frac{\partial n_{Pl}}{\partial T}$$

$$= y \, \frac{x e^x}{(e^x - 1)^2} \left(x \frac{e^x + 1}{e^x - 1} - 4 \right)$$

$$\Delta I_{sz} = I_{sz} - I_{planck} = \frac{2 h \nu^3}{c^2} n_{sz}$$

